Austrian Journal of Earth Sciences | Vienna | 2015 | Volume 108/2 | 245 - 276 | DOI: 10.17738/ajes.2015.0025

Depositional environment and provenance analyses of the Zöbing Formation (Upper Carboniferous-Lower Permian), Austria

Slavomír NEHYBA[1)*)] & Reinhard ROETZEL[2)]

[1)] Institute of Geological Sciences, Faculty of Science, Masaryk University, Kotlářská 2, CZ- 611 37 Brno, Czech Republic;

[2)] Geological Survey, Neulinggasse 38, A-1030 Wien, Austria;

[*)] Corresponding author, slavek@sci.muni.cz

KEYWORDS Zöbing Formation; Upper Carboniferous-Lower Permian; facies and provenance analyse; terrestrial deposits; terminal fluvial system

Abstract

The deposits of the Upper Carboniferous to Lower Permian Zöbing Formation in Lower Austria have been studied by a wide range of sedimentological methods in several limited outcrops. Four facies associations were identified: (a) non-channelized fine-grained deposits; (b) channelized sandstones, (c) non-channelized conglomerates, and (d) channelized conglomerates. Non-channelized fine-grained sediments are interpreted as deposits in shallow, semi-permanent pools on floodplains. Channelized sandstones are associated with fluvial processes and mostly represent crevasse channels cut into the floodplains. Channelized conglomerates originated from coarse-grained confined and hyperconcentrated flows. Non-channelized conglomerates are interpreted as sediments of alluvial fan and alluvial plain systems. A terminal fluvial system developed under a semi-arid to arid climatic regime is supposed to be the depositional environment of the Zöbing Formation.

The detritus was mostly derived from primary sources formed by crystalline rocks. The proportion of metamorphites (particularly metapelitic rocks, such as mica schists, paragneisses, felsitic granulites) was predominant along with acidic magmatic and volcanic rocks. The source area predominantly can be located in the Moldanubian unit. Rapid physical erosion, redeposition and subordinately also chemical weathering are all supposed in the source area. The general provenance evolution of the entire Zöbing Formation shows local/adjacent sources in the basal parts whereas a wider provenance and variations in the primary and recycled detritus are assumed for the younger parts of the succession.

1. Introduction

The late Variscan period in Central Europe was a period of intense tectonic, magmatic and sedimentary activity. Subsequent to the Variscan Orogeny during the Westphalian basin formation took place in the Stephanian-Autunian in both the internal and external Variscides. Approximately 70 basins developed in the Western and Central Europe within a relatively short time span (McCann et al., 2006). Most of these basins trace long-lived Variscan fault systems. In the internal parts of the Variscan orogen the basins tend to be relatively small, deep and isolated commonly of graben or half-graben type. Small isolated grabens were relatively fast filled by mainly locally derived sediments and associated volcaniclastic rocks, which led to the accumulation of thick sequences of terrestrial deposits termed Rotliegendes. The filling of the basins generally coincided with an overall change to semi-arid climate (Stephanian–Early Permian). Small isolated grabens with terrestrial infill represent a challenge for basin to basin stratigraphic correlations (McCann et al., 2006).

Similarly the continental Permo-Carboniferous basins of the Bohemian Massif record a long history of post-Variscan extensional collapse from the Westphalian up to the Early Triassic (Kalvoda et al., 2008). The erosional remnants of these deposits, like in the Boskovice Basin in the Czech Republic and the Zöbing area in Austria, provide data not only about the post-orogenic depositional history but also about paleogeography and the climatic and tectonic events (Nehyba et al., 2012). The preorogenic and synorogenic facies development in this area is reflected by Devonian and Carboniferous sediments like the limestone of the Moravian Karst or the Variscan Flysch ("Culm facies") in the area between Brno and Ostrava (Kalvoda et al., 2008).

In the surroundings of Zöbing a succession of Upper Carboniferous to Permian sediments is exposed in an area of about 5.5 km^2. These deposits represent a relic preserved on the southernmost margin of the Bohemian Massif, which make them interesting in relation to the Upper Paleozoic deposits of the Eastern Alps (Krainer, 1993). Unfortunately, the rhyolithic rock fragments in the Zöbing Formation were not absolutely dated until now to allow a direct correlation.

The small areal extent and poor exposure led to a low attractiveness of the Zöbing Formation for geological studies so far. Moreover, the structure of the basin has been obscured by younger tectonic events.

The main intention of this paper is to provide reliable information about the evolution of the local basin in which the Zöbing Formation was deposited using complex data from several small isolated exposures. A simplified map of the studied area is presented in Fig. 1.

2. Regional geological setting

In the surroundings of Zöbing a more than 1000 m thick succession of Upper Carboniferous to Permian sediments occur in

an approximately 6.5 km long and up to 2.3 km wide wedge-shaped area, which mainly crop out at the Heiligenstein east to southeast of Zöbing and extend as far as Elsarn and Olbersdorf in the northeast (Fig. 1). These deposits of the Zöbing Formation (ZF) are well known since the 19th century (cf. Holger, 1842; Partsch, 1843, 1844; Čžjžek, 1849, 1853; Ettingshausen, 1852; Stur, 1870; Suess, 1912; Waldmann, 1922; Vohryzka, 1958; Schermann, 1971). The last detailed mapping was done by Vasicek (1974, 1975), who also defined the Zöbing Formation and divided it into several members (Vasicek, 1991a; cf. Vasicek, 1977, 1983, 1991b; Vasicek and Steininger, 1996). From the Zöbing Formation plant fossils were described by Berger (1951), Vasicek (1977, 1983, 1991a, b) and Vasicek and Steininger (1996) (cf. Tenchov, 1980; Cichocki et al., 1991). Bachmayer and Vasicek (1967) described remains of insects, Flügel (1960) non-marine molluscs and Schindler and Hampe

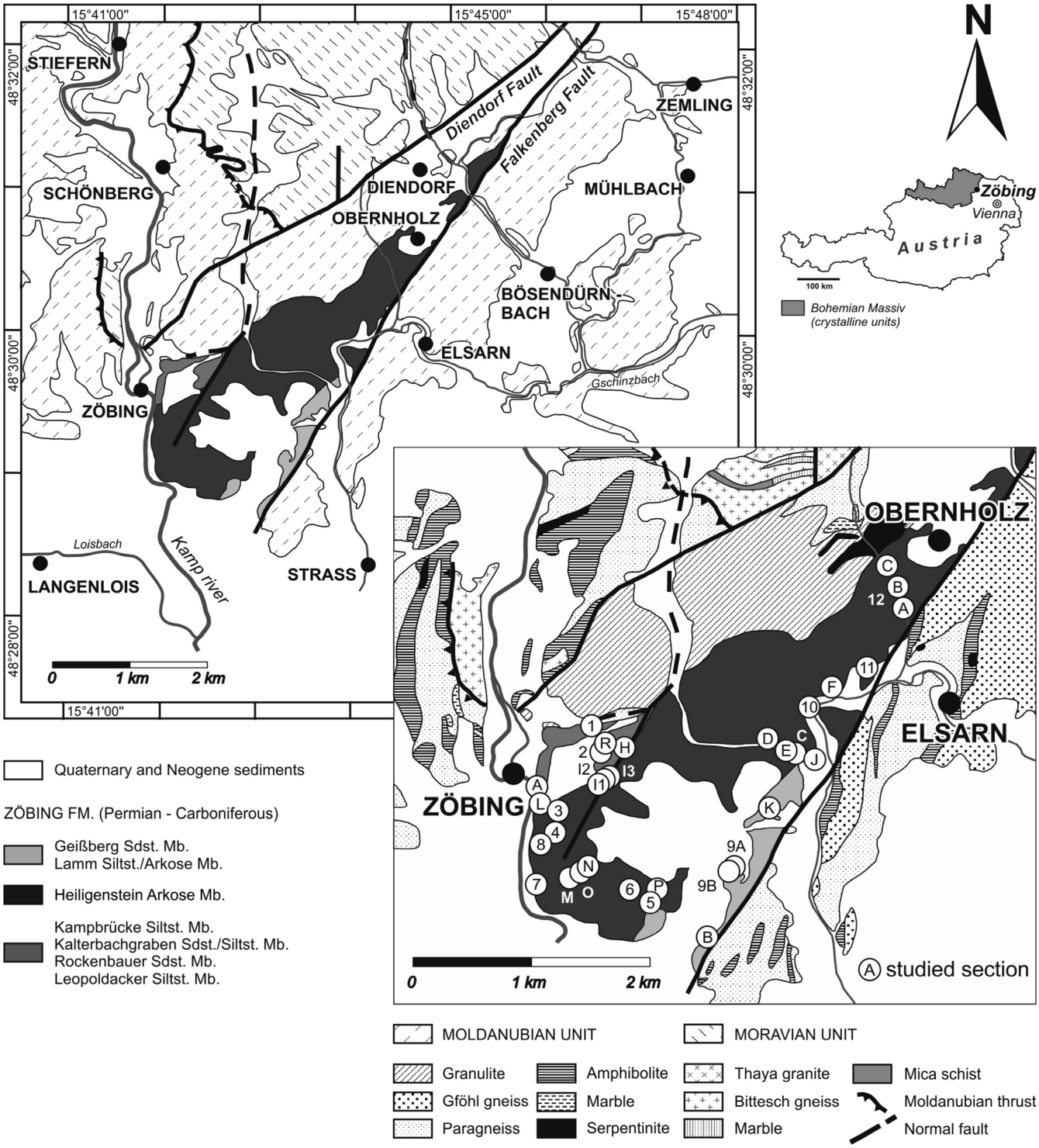

Figure 1: Schematic geological maps of the investigated area and position of studied sections (maps compiled from Fuchs et al., 1984; Frasl et al., 1991; Heinrich et al., 2008).

(1996) remains of fish. However, until now no detailed sedimentological study was done.

The sediments of the Zöbing Formation are tectonically tilted together with the crystalline basement (mainly granulite and ultrabasic rocks) and preserved in a tectonic graben between the Diendorf fault in the northwest and the Falkenberg fault in the southeast (Waldmann, 1922; Fuchs et al., 1984). At present crystalline rocks of the Moldanubian unit (granulite, Gföhl gneiss, mica schists, amphibolite) are exposed in the surroundings of the Permocarboniferous sediments. North of the exposures of the Zöbing Formation also granites, Biteš gneiss und mica-schists of the Moravian unit are located close to the Paleozoic sediments.

The succession of the Zöbing Formation can be divided into three parts (Fig. 2). The crystalline basement is unconformably overlain by the basal part of the Zöbing Formation in the southwest with an about 300 m thick succession of alternating silt- and sandstones, which can be divided into four members.

The lowermost *Leopoldacker Siltstone Member* mainly consist of dark grey, fine-grained, laminated silt- and sandstones with small coal seams and a high amount of organic remains. In coaly shales and coal-streaks close to the base a well preserved flora with Late Carboniferous ferns and horsetails occur (Vasicek, 1983, 1991a, b; Vasicek and Steininger, 1996). Siltstones contain freshwater bivalves (Flügel, 1960) and in dark grey carbonate nodules ("coal balls") freshwater gastropods, ostracods, and small fish teeth and fish scales (Schindler and Hampe, 1996) were found.

The overlying ochre-brown, thin bedded and slightly calcareous silt- to sandstones of the *Rockenbauer Sandstone Member* upward grade into thin laminated carbonaceous shales ("Brandschiefer"). The sediments contain often resedimented clay- and sandstone-pebbles and remains of conifers (Vasicek, 1983, 1991a, b; Vasicek and Steininger, 1996). Ostracods, teeth and coprolites of fish and a fragment of an insect wing were found in this member (Schindler and Hampe, 1996).

The *Kalterbachgraben Sandstone/Siltstone Member* above is composed of alternating massive layers of partly arkosic sandstones with dark grey, laminated silt- to sandstones (Vasicek, 1983, 1991a, b; Vasicek and Steininger, 1996). In this succession dark, laminated limestones, reddish siltstones, a coal seam, and a thin layer of rhyolitic tuff (Schindler and Hampe, 1996) are intercalated. Fossils were only found in an individual limestone bed, from where Schindler and Hampe (1996) described many ostracods and few fish teeth.

The topmost member of the basal succession is the *Kampbrücke Siltstone Member*, which consist mainly of layered siltstones alternating in longer intervals with arkosic sandstones and two fossil-bearing horizons. In the lower fossiliferous horizon a rich flora with ferns and horsetails (Vasicek, 1974, 1977, 1983) occur, whereas the higher horizon contains remains of conifers, freshwater bivalves, and insect wings (Bachmayer and Vasicek, 1967; Vasicek, 1991b).

The middle part of the Zöbing Formation is approximately

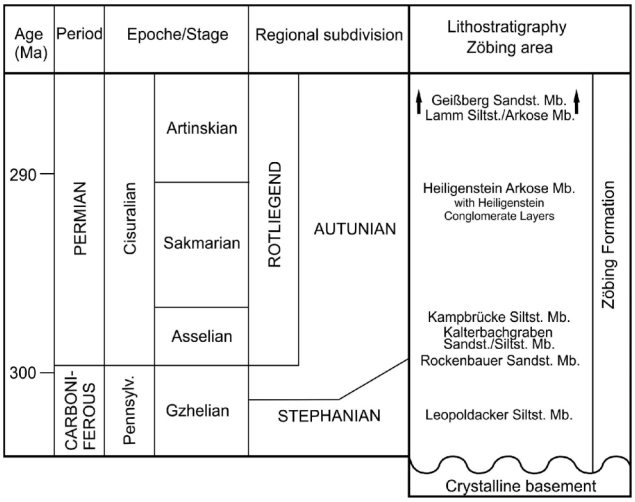

Figure 2: Lithostratigraphic correlation of the Upper Carboniferous – Permian sediments in the Zöbing area (Vasicek, 1991a; Nehyba et al., 2012).

OUTCROP	LAT-WGS84	LONG-WGS84
A	48,491540	15,69790
B	48,48030	15,71810
C	48,494430	15,727630
D	48,495410	15,724410
E	48,494480	15,726550
F-A	48,49940	15,731770
F-B	48,499440	15,731980
H	48,494610	15,707930
I-1	48,492160	15,705970
I-2	48,492220	15,70610
I-3	48,492470	15,706330
J	48,493820	15,729840
K	48,490120	15,724730
L	48,490370	15,698270
M	48,484480	15,701760
N	48,485290	15,703860
O	48,484930	15,703020
P	48,483670	15,711860
R	48,495100	15,706000
1	48,496290	15,704130
2	48,494250	15,705240
3	48,489680	15,700370
4	48,48800	15,700060
5	48,482620	15,711050
6	48,483630	15,708670
7	48,483960	15,697930
8	48,487070	15,698390
9A	48,485450	15,720720
9B	48,48510	15,720330
10	48,497880	15,729010
11	48,500980	15,735790
12A	48,505590	15,739950
12B	48,507240	15,739280
12C	48,508870	15,738030

Table 1: List of studied outcrops of the Zöbing Formation with coordinates in WGS84 system. For position of the outcrops refer to Fig. 1.

700 m thick and includes the *Heiligenstein Arkose Member*, which consists of an alternation of arkosic sandstones and conglomerates. The grain size of this member increases towards the top, where conglomerates (*Heiligenstein Conglomerate Layers*) predominate.

The conglomerates are composed mainly of granulite, subordinately also quartz, quartzite, granitic gneisses, amphibolites, marble, Gföhl gneiss, and clasts of rhyolite (Waldmann, 1922; Vohryzka, 1958; Schermann, 1971; Vasicek, 1977, 1991b). Boulders in these conglomerates are up to 1 m in diameter.

Above the Heiligenstein Arkose Mb. the third, about 400 m thick upper part of the Zöbing Formation starts with the *Lamm Siltstone/Arkose Member*. It shows an alternation of reddish-brown siltstones and arkosic sandstones. In finer parts of the succession intercalations of dark grey silicified limestones can be observed (Vasicek, 1983, 1991a, b; Vasicek and Steininger, 1996). From pelitic sediments Vasicek (1991b) described imprints of raindrops. In the uppermost part of the Zöbing Formation the *Geißberg Sandstone Member* occurs, which is a succession of red and grey claystones in alternation with arkosic sandstones (Vasicek, 1983, 1991a, b; Vasicek and Steininger, 1996).

The sediments of the Leopoldacker Siltstone Mb. at the base of the Zöbing Formation are dated by the seed fern *Alethopteris zeilleri* and similar forms to the Late Carboniferous (Stephanian) (Vasicek, 1977, 1983, 1991a; Vasicek and Steininger, 1996). In the overlying Rockenbauer Sandstone Mb. and Kampbrücke Siltstone Mb. callipterids like the seed fern *Callipteris conferta*, the conifer *Ernestiodendron filiciformis* and fructifications of horsetails (*Calamostachys dumasii*) already point to an Early Permian (Autunian) age (Schindler and Hampe, 1996; Vasicek and Steininger, 1996). Rhyolitic volcanic clasts in the Heiligenstein Arkose Mb. are correlated with the volcanic activity related to the Middle Permian "Saalic orogenic phase" (Vasicek, 1977, 1983, 1991a, b; Vasicek and Steininger, 1996).

For the basal, fine-grained part of the Zöbing Formation Schindler and Hampe (1996) assume as depositional environment shallow eutrophic lakes with a vegetation-rich riparian zone or stagnating oxbow lakes close to a fluvial environment. Near the base of the Kalterbachgraben Sandstone/Siltstone Mb. a climatic change to more arid conditions starts which caused also a change in the depositional environment. The arkoses and conglomerates of the Kalterbachgraben Sandstone/Siltstone Mb. and the Heiligenstein Arkose Mb. are interpreted as periodic flash-flood deposits in arid alluvial environments of the Permian (Vasicek, 1991a, b).

3. Methods

The presented results are based on the study of ZF outcrops. The ZF is poorly exposed mostly along creeks and ravines, road

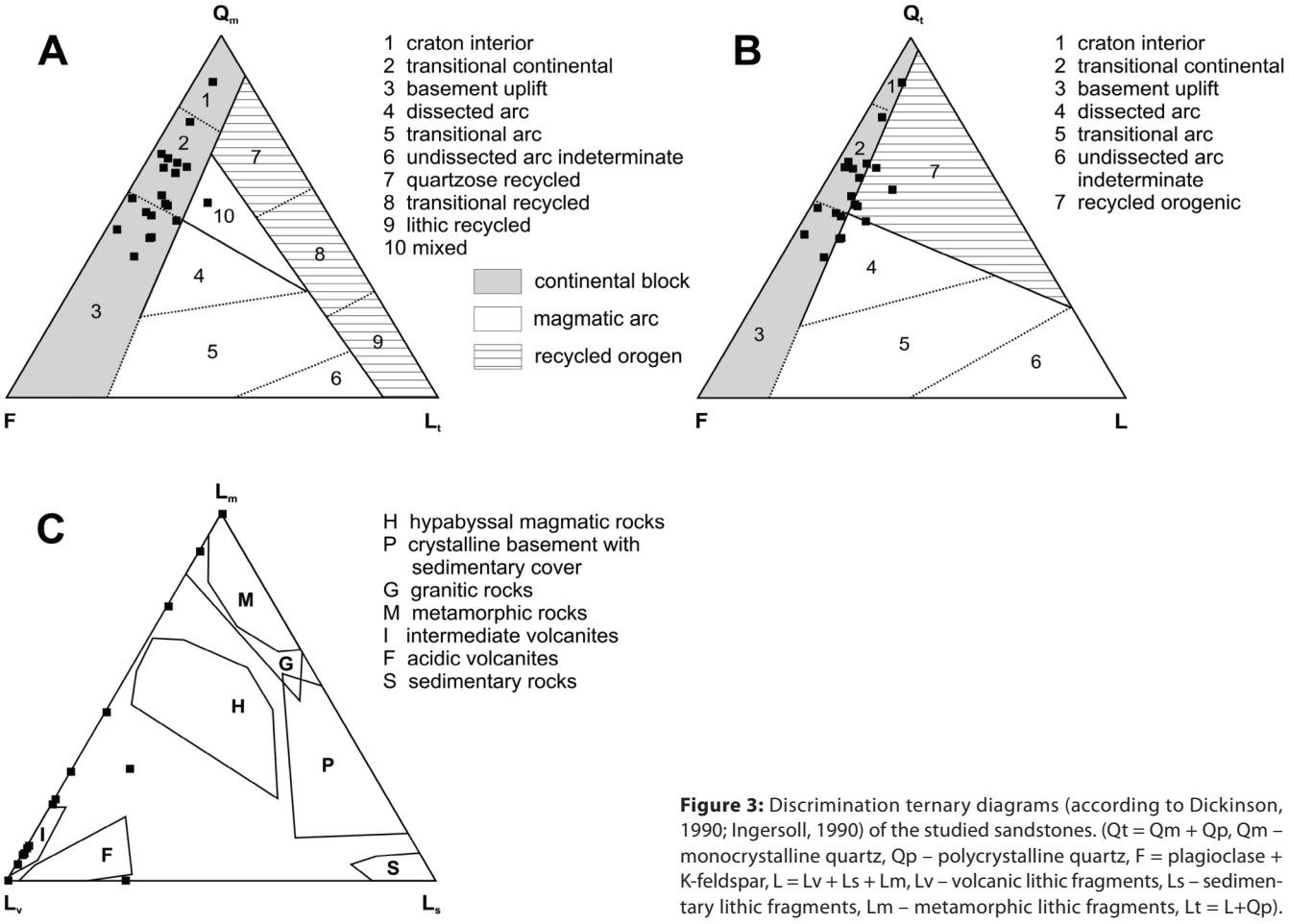

Figure 3: Discrimination ternary diagrams (according to Dickinson, 1990; Ingersoll, 1990) of the studied sandstones. (Qt = Qm + Qp, Qm – monocrystalline quartz, Qp – polycrystalline quartz, F = plagioclase + K-feldspar, L = Lv + Ls + Lm, Lv – volcanic lithic fragments, Ls – sedimentary lithic fragments, Lm – metamorphic lithic fragments, Lt = L+Qp).

cuttings and small quarries. The lateral extent of these outcrops is typically limited to a few metres and similarly reduced are the vertical sections. A list of outcrops is shown in Tab. 1.

The outcrops were studied by a mix of reconnaissance-scale and detailed sedimentary logging. The sedimentary facies were studied by logging, with local paleocurrent directions measured from foresets, channel axis or imbricate gravel fabric (according to Collinson and Thompson, 1982). The depositional architecture has been studied in 2D outcrop sections by a line-drawing of stratification and bedding traces on outcrop photomosaics.

Samples for provenance analyses were only selected from sandstone bedforms. The framework grains were point counted in 20 thin sections according to the standard method (Dickinson and Suczek, 1979; Dickinson and Valloni, 1980; Zuffa, 1980, 1985; Ingersoll, 1990). The entire rock geochemistry was evaluated in the ACME laboratories Vancouver, Canada (23 analyses).

Heavy minerals were studied in the grain-size fraction 0.063-0.125 mm in 23 samples. Garnet, zircon, and rutile represent the most common heavy minerals in the studied deposits, being relatively stable during diagenesis and having a wide compositional range, so as to be further evaluated in detail along with spinel. The outer morphology, colour, presence of older cores, inclusions, and zoning were evaluated in the entire zircon spectra (419 grains). Only the euhedral or subhedral zircons were considered in the study of typology (86 grains) and elongation (170 grains). The electron microprobe analysis of garnet (347 grains), rutile (139 grains), and spinel (10 grains) was evaluated with a CAMECA SX electron microprobe analyser (Faculty of Science, Masaryk University, Brno, Czech Republic).

The paleocurrent results are based on measurements of the orientation of channel axes (11), foresets of cross-stratification (41), preferred orientation of elongated pebbles (17), and accretional surfaces (18). The effect of tilting was removed by the Spheristat program (Stesky, 1998). The rose diagrams were constructed according to Nemec (1988) using the EZ-Rose computer program of Baas (2000).

4. Results

4.1 Petrography

Sandstones are in general coarse- to medium-grained, often texturally immature and poorly sorted with a certain admixture of granules. The sandy grains are often angular and sub-angular, whereas small pebbles are usually rounded.

The sandstones contain a significant amount of both mono- and polycrystalline quartz. The anhedral quartz grains indicate the origin from granitoids. Cataclasis of grains was common. Subhedral to euhedral feldspar grains (commonly partly altered) are mostly less common than quartz grains. Plagioclases often dominate over alkali feldspars. The clasts derived from fine-grained acidic plutonites, fine-grained gneisses and granulites were determined regularly, whereas clasts of quartzites were rare. Rare acidic volcanic rock fragments with

Member of ZF	Dominant heavy minerals	Additional heavy minerals	ATi ratio	GZi ratio	RZi ratio	ZTR index
Rockenbauer Sandstone Mb.	rutile (72.1%), zircon (14.7%)	apatite, titanite, zoisite, epidote, monazite, garnet, staurolite, tourmaline, andalusite	33.3	19.7	19.7	87.8
Kalterbachgraben Sandstone/Siltstone Mb.	garnet (73.4%), rutile (15.2%)	zircon, kyanite, apatite, titanite, monazite	100	91.2	68.2	22.3
Kampbrücke Siltstone Mb.	garnet (60.4%), rutile (9.4%)	zircon, apatite, zoisite, monazite, staurolite, tourmaline, anatase, kyanite, andalusite	100	94.1	71.2	13.2
Heiligenstein Arkose Mb.	garnet (78.6-85.0%)	rutile, apatite, zircon, staurolite, monazite, zoisite, kyanite	100	82.4-98.9	70.6-92.8	3.2-8.8
Heiligenstein Arkose Mb.	garnet (30.6-63.3%), rutile (7.4-19.8%), apatite (1.7-22.2%), zircon (5.5-33.2%)	staurolite, monazite, zoisite, tourmaline, epidote, andalusite, kyanite	83.5-100	52.0-91.0	33.0-69.3	12.9-46.8
Heiligenstein Arkose Mb.	rutile (16.3-34.7%), zircon (12.6-19.0%), garnet (18.1-23.0%), apatite (16.2-36.8%)	spinel, sillimanite, monazite, titanite, andalusite, kyanite, staurolite, tourmaline, epidote	98.9-100	48.8-64.6	56.4-64.6	29.3-53.7
Lamm Siltstone/ Arkose Mb. and Geißberg Sandstone Mb.	garnet (54.1-84.9%), zircon (6.8-22.6%), apatite (5.0-19.9%), rutile (2.0-10.3%)	kyanite, sillimanite, epidote, andalusite, tourmaline, monazite, titanite, staurolite, spinel	82.9-100	70.5-99.0	13.1-82.0	5.0-26.7

Table 2: Heavy mineral assemblages and mineral ratios of individual members of the Zöbing Formation.

micropoikilitic structures point to an acidic volcanic source. Garnet, cordierite, rutile, tourmaline, and zircon were identified as accessory minerals. The amount of matrix varies between 4 to 44%. Diagenetically formed sericite and chlorite, together with detrital micas (both biotite and muscovite) were recognised in the matrix. Cement, which often intensively colours the matrix, is formed by sparitic and microsparitic calcite and amorphous Fe oxi-hydroxides. Carbonates sometimes replace detrital grains. Sandstones can be mainly classified (according to Pettijohn et al., 1987) as lithic greywackes (89%), less common are litharenites (11%). No significant differences were recognised between samples from different members of the Zöbing Formation.

On the Q_m-F-L_t (Fig. 3a) discrimination diagram the majority of the samples from the ZF occupy the continental block field. This correlation is also supported by the position in the Qt-F-L diagram (Fig. 3b). The position of the samples in the L_m-L_v-L_s diagram (Fig. 3c) (Ingersoll, 1990) points to a source from crystalline rocks and also to a significant portion of volcanics in the source area. On the ternary discriminating diagram (Dickinson and Valloni, 1980; Dickinson, 1990) the sandstones of the ZF plot in the field of the basement uplift of the stable craton.

4.2 Heavy mineral studies

Heavy minerals are sensitive indicators for provenance, weathering, transport, deposition, and diagenesis, in particular when the study of assemblages and the ratios of the abundance of minerals with similar hydraulic and diagenetic behaviour (Morton and Hallsworth, 1994) are combined with the chemistry of selected heavy minerals (Morton, 1985, 1991). The heavy mineral ratios apatite/tourmaline (ATi), garnet/zircon (GZi), TiO_2-group/zircon (RZi), and the ZTR (zircon+tourmaline+rutile) index have been used. ATi, GZi and RZi provide a solid reflection of the source rocks characteristics being comparatively immune to alteration (Morton and Hallsworth, 1994). The ZTR index is widely accepted as a criterion for the mineralogical „maturity" (Hubert, 1962; Morton and Hallsworth, 1994).

4.2.1 Heavy mineral assemblages and mineral ratios

Some differences were recognised in the heavy mineral assemblages of various members of the Zöbing Formation but significant differences existed also between individual beds of the members. The results are presented in Tab. 2.

Two associations were determined in the samples from the Heiligenstein Arkose Mb. Basal deposits (Rockenbauer Sandstone Mb.) are typified by a predominance of rutile and zircon, show low ATi and GZi-ratios, a high RZi-ratio and ZTR index. The higher part of the succession (Kalterbachgraben Sandstone/Siltstone Mb., Kampbrücke Siltstone Mb., Heiligenstein Arkose Mb., Lamm Siltstone/Arkose Mb., and Geißberg Sandstone Mb.) are characterised especially by increased amounts of garnet. Rutile, zircon, and apatite are also significantly present in some samples.

4.2.2 Rutile

Medium- to high-grade metamorphic rocks are considered to be the main primary source of detrital rutile (Force, 1980) and so the mineral is attractive for provenance analyses (Zack et al., 2004a, b; Triebold et al., 2007).

The concentration of the main diagnostic elements (Fe, Nb, Cr, and Zr) varies significantly in the studied samples. The concentration of Nb ranges between 412 and 9520 ppm (average 2045 ppm), the concentrations of Cr vary between 3 and 3480 ppm (average 1067 ppm), of Zr between 70 and 7706 ppm (average 2697 ppm), and the value of logCr/Nb is mostly negative (87.5%). The discrimination plot Cr vs. Nb is presented in Fig. 4. The majority of rutiles originate from metapelitic rocks (62.9%), whereas less common is the origin from metamafic rocks (19.1%) and pegmatites (18%). The Zr-in-rutile thermometry was applied for metapelitic zircons only (for a stable rutile-quartz-zircon assemblage cf. Zack et al., 2004 a, b; Meinhold et al., 2008). The results indicate that 92.3% of metapelitic rutiles were derived from rocks of granulite metamorphic facies and 7.7% from amphibolite/eclogite facies. No significant differences in rutile chemistry were recognised between samples from different members of the Zöbing Formation.

4.2.3 Garnet

The chemistry of detrital garnet is widely used for the determination of provenance (Morton, 1991). The results of the analyses are presented in the Tab. 3.

The garnet composition of all lithostratigraphic members of the ZF is surprisingly monotonous. Almandine is absolutely predominating as pyrope-almandines comprise 93.9% of the spectra. Almandines form 2.2%, grossular-pyrope-almandines 1.9%, spessartine-almandines 1.4%, and grossular-almandines 0.7%. Exceptional are pyrope-andradite-alman-

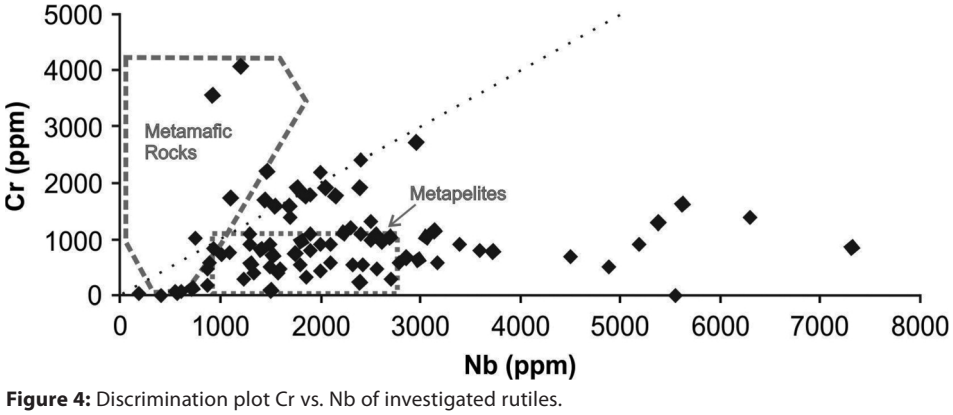

Figure 4: Discrimination plot Cr vs. Nb of investigated rutiles.

Garnet type	Frequency
$ALM_{(82-90)}$	2.2%
$ALM_{(49-83)}$-$PRP_{(11-48)}$	93.9%
$ALM_{(62-64)}$-$PRP_{(18-25)}$-$GRS_{(10-15)}$	1.9%
$ALM_{(60-67)}$-$GRS_{(19-34)}$	0.7%
$ALM_{(50-83)}$-$SPS_{(14-42)}$	1.4%
$GRS_{(66-89)}$-$AND_{(11-31)}$	0.3%
$GRS_{(82-84)}$	0.3%

Table 3: Garnet types of the studied ZF deposits (ALM: almandine, GRS: grossular, PRP: pyrope, SPS: spessartine, AND: andradite, $_{(50-75)}$ - proportional representation of the garnet type).

dine and grossular.

4.2.4 Zircon

The evaluation of the outer morphology/shape of zircon can be used for the determination of its source rocks and first-cycle detritus or recycling (Poldervaart, 1950; Mader, 1980; Winter, 1981; Lihou and Mange-Rajetzky, 1996).

The subrounded and rounded zircons comprised 38.8% of the studied samples whereas subhedral grains formed 44.4% and euhedral zircons 16.8%. Certain differences in the shape of zircons were recognised between deposits of various members of the Zöbing Formation. The highest occurrence (i.e. 51.9-73.9%) of subrounded and rounded zircons was recognised in the lower members (i.e. Rockenbauer Sandstone Mb. and Kalterbachgraben Sandstone/Siltstone Mb.) whereas the highest occurrence of euhedral zircons was observed in the higher members (i.e Heiligenstein Arkose Mb. and Lamm Siltstone/Arkose Mb.).

Zircons with a pale colour predominate, forming 52.8% while colourless zircons constitute 34.1% of the spectra. Zircons with a brown colour form 7.2%, opaque ones 0.2% and pink zircons 0.7%.

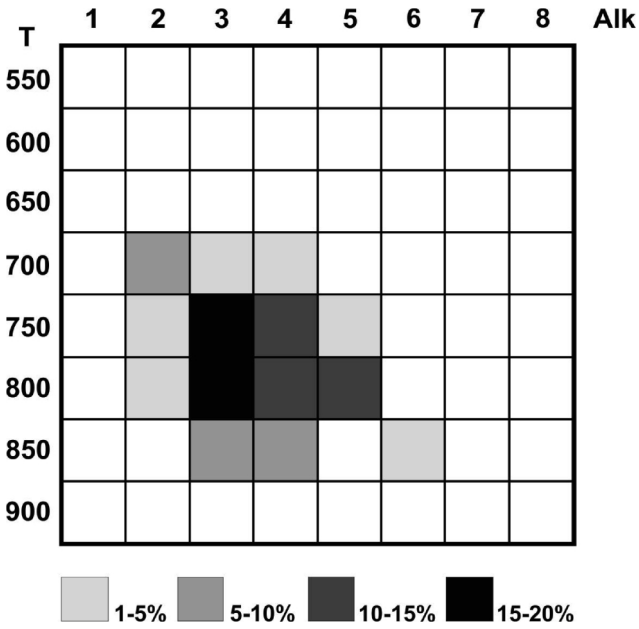

Figure 5: Typology of zircons in the Pupin-diagram (Pupin, 1980).

The proportion of zoned zircons forms a maximum of 8.4% and zircons with older cores 5.7%. All the studied zircons show inclusions.

Elongation of zircons (the relationship between the length and width of the crystals) can help to trace back the source (Poldervaart, 1950; Zimmerle, 1979; Winter, 1981). The average value of elongation was 2.31. Zircons with elongation above 2.0 predominate with 62.9 %. Zircons with an elongation of more than 3 represent 15.6%. Such zircons are supposed to reflect a magmatic/volcanic origin (Zimmerle, 1979) and/or only limited transport. The maximum elongation was 5.5. Any significant differences in the value of elongation were recognised between samples from various members of the Zöbing Formation.

Zircon typology can provide data regarding the parental magma and so can be used for tracing the precise provenance (Pupin, 1980, 1985; Finger and Haunschmid, 1988, etc.). The parental magmas of the studied zircons had a hybrid character (close to the anatectic origin) in accordance with the position of the "typology mean point" (Pupin, 1980, 1985). The predominance of the typological subtypes S17 and S12 of Pupin (1980) can be observed in the ZF (Fig. 5). A slightly higher occurrence of subtype S12 seems to be present in the Kalterbachgraben Sandstone/Siltstone Mb. whereas a slightly higher appearance of S 17 seems to be connected with the Heiligenstein Arkose Mb.

4.2.5 Spinel

Although spinel was particularly rare in the studied heavy mineral assemblages, its microprobe study reveals that 70% of spinels have a higher content of Cr (>2500 ppm). These spinels can be classified as chromian ones, which are a typical mineral for peridotites and basalts (Pober and Faupl, 1988) reflecting a source from mafic/ultramafic rocks. The plot of TiO_2 against Al_2O_3 (Fig. 6) for spinels fits more for a volcanic source, which also suggests the relatively high TiO_2 concentrations (Kamenetsky et al., 2001; Zimmermann and Spalletti, 2009).

4.3 Major element geochemistry

The positive correlation of Al_2O_3 with TiO_2, Fe_2O_3, K_2O, and MgO (Fig. 7a) suggests that chemical weathering in the source area was an important factor controlling the mineralogy of weathered products. The trends in Al_2O_3 and TiO_2 contents are almost consistent and indicate either similar provenance or weathering and depositional history for the deposits. (Young and Nesbitt, 1998; Passchier and Whitehead, 2006). The vertical distribution of the samples reflects a mixing of sands and muds during deposition, whereas the horizontal distribution reflects different weathering and sorting of the sand fraction. The studied deposits reveal relatively low Al_2O_3 and TiO_2 values, characteristic for granulites and granitoids (Passchier and Whitehead, 2006). Significant enrichment in Al with respect to average crystalline rocks (due to weathering) was not determined (Passchier and Whitehead, 2006), but the average content of Al_2O_3 is 11.7% and 43% of samples are relatively

enriched in Al_2O_3 (above 12%) probably caused by the matrix rich in kaolinite. The Ti:Al ratio varies between 0.01-0.07 (average 0.04). Relatively low TiO_2 and Al_2O_3 concentrations can be partly explained by grain-size effect (Young and Nesbit, 1998; Passchier, 2004).

The plot of TiO_2/Zr – Zr/Al_2O_3 (Fig. 7b) illustrates, that the data follow similar patterns and point to a similar provenance (Passchier and Whitehead, 2006).

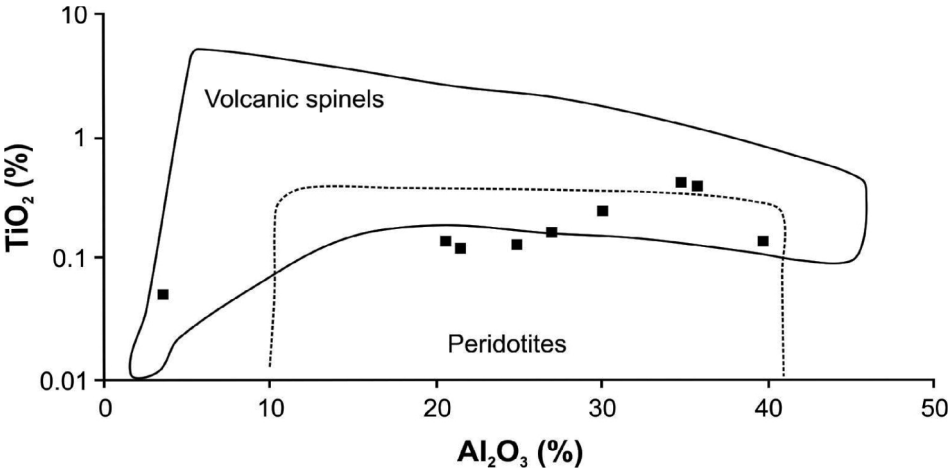

Figure 6: Discrimination plot of TiO_2 vs. Al_2O_3 for investigated spinels.

The value of the ratio K_2O/Na_2O (Roser and Korsch, 1986) for the studied sediments varies between 0.31 and 3.3 (average 1.16). Such relatively low values reflect a derivation from mainly primary sources and a highly varied portion of recycled sedimentary sources (McLennan et al., 1993; Bock et al., 1998). Higher ratios (above 1) can reflect a derivation from recycled sedimentary sources with an extended weathering history (Roser and Korsch, 1986). Such samples are about 50%. Similarly, the K_2O/Al_2O_3 ratio can be used to estimate the degree of recycling (Cox and Lowe, 1995, Passchier, 2004). Its value is between 0.08 and 0.37 (average 0.23). The relatively low ratios could indicate a source from quartz-rich rocks and the significant variations of the ratio point to a variation in the content of recycled sediments. Typically, a sample from the Rockenbauer Sandstone Mb. reveals the lowest value of recycling. However, because of the relatively easy affection of the alkali elements during weathering and diagenesis, the use of alkali elements could be problematic.

The studied samples are sedimentary rocks from heteroge-

Sample	%										
	SiO_2	Al_2O_3	Fe_2O_3	MgO	CaO	Na_2O	K_2O	TiO_2	P_2O_5	MnO	Cr_2O_3
ZP 1	80.00	10.93	1.47	0.53	0.27	2.45	3.89	0.20	0.11	0.01	0.006
ZP 2	76.87	11.93	2.99	1.22	0.36	2.55	3.41	0.33	0.13	0.07	0.018
ZP 3	77.29	11.34	2.24	1.16	1.11	2.99	3.17	0.30	0.22	0.03	0.009
ZP 4	70.85	14.83	4.28	2.69	1.21	2.15	3.11	0.55	0.16	0.04	0.012
ZP 5	77.53	12.03	1.55	0.79	0.22	2.92	4.40	0.18	0.12	0.03	0.014
ZP 6	71.68	14.02	3.60	2.05	0.61	3.98	3.11	0.41	0.18	0.05	0.012
ZP 7	82.66	9.37	3.41	0.80	0.43	0.55	1.81	0.58	0.14	0.06	0.034
ZP 8	79.88	9.81	4.27	1.43	0.34	2.59	0.83	0.57	0.10	0.02	0.034
ZP 9	76.59	12.45	2.15	0.86	0.36	2.73	4.30	0.29	0.15	0.03	0.011
ZP 10	75.62	12.75	2.99	1.28	0.35	2.42	3.86	0.35	0.15	0.11	0.010
ZP 11	81.34	10.44	1.36	0.36	0.11	2.21	3.75	0.25	0.07	0.01	0.006
ZP 12	81.65	9.53	1.60	0.33	1.75	2.80	1.86	0.13	0.09	0.17	0.004
ZP 13	78.09	11.31	3.98	1.56	0.55	2.65	1.10	0.38	0.20	0.02	0.045
ZP 14	77.57	11.44	4.32	1.73	0.55	2.55	1.15	0.36	0.19	0.02	0.043
ZP 15	77.11	12.13	4.02	1.74	0.51	2.29	1.50	0.42	0.17	0.04	0.038
ZP 16	74.48	9.11	1.36	0.77	5.13	1.73	2.52	0.16	0.09	0.08	0.003
ZP 17	74.35	11.75	4.68	1.30	0.50	1.93	3.40	0.56	0.10	0.05	0.011
ZP 18	74.39	12.52	2.33	1.06	0.25	3.83	3.46	0.44	0.12	0.03	0.011
ZP 19	75.69	10.71	3.99	1.11	1.97	3.12	1.01	0.26	0.10	0.09	0.007
ZP 20	59.63	16.97	6.97	3.28	0.71	3.58	3.06	0.86	0.23	0.03	0.020
ZP 21	69.97	13.11	3.76	2.25	1.96	2.93	1.80	0.49	0.14	0.04	0.009
ZP 22	61.50	13.61	4.11	1.93	5.74	4.03	2.44	0.62	0.27	0.09	0.014
ZP 23	67.82	14.77	5.21	1.66	0.49	2.86	3.64	0.62	0.15	0.04	0.013
ZP 24	65.11	14.01	3.95	2.02	3.51	2.59	2.93	0.59	0.25	0.07	0.010
ZP 25	63.73	12.01	2.02	1.55	7.31	2.66	2.53	0.35	0.15	0.13	0.006
ZP 26	81.81	8.95	1.42	0.57	0.25	1.90	3.32	0.17	0.08	0.02	0.009

Table 4: The major element composition (%) of studied samples.

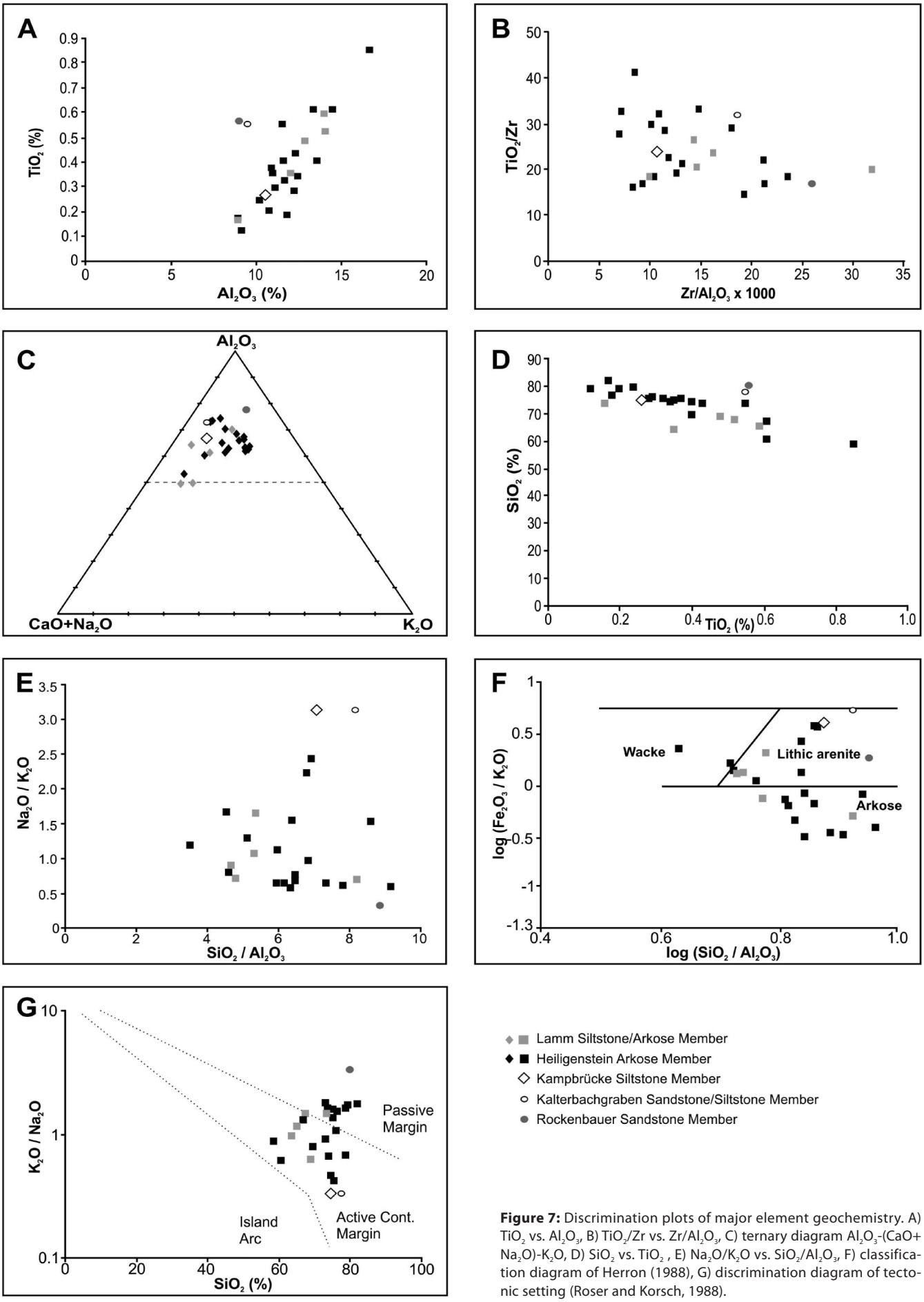

Figure 7: Discrimination plots of major element geochemistry. A) TiO_2 vs. Al_2O_3, B) TiO_2/Zr vs. Zr/Al_2O_3, C) ternary diagram Al_2O_3-(CaO+Na_2O)-K_2O, D) SiO_2 vs. TiO_2 , E) Na_2O/K_2O vs. SiO_2/Al_2O_3, F) classification diagram of Herron (1988), G) discrimination diagram of tectonic setting (Roser and Korsch, 1988).

neous source rocks and have undergone sorting during transportation in fluvial channels. The weathering indices could reflect variations in parent rock composition rather than the degree of weathering (Borges and Huh, 2007). Commonly used is the chemical index of alteration (CIA index – Nesbitt and Young, 1982), although due to the highly varying carbonate content and lack of CO_2 data, a precise correction for the carbonate CaO was difficult. After correcting for P_2O_5 (apatite), the value of CaO is consequently accepted, if the mole fraction of CaO ≤ Na_2O. However, if CaO ≥ Na_2O, it was assumed, that the moles of CaO=Na_2O (McLennan et al., 1993). The CIA index ranges between 49 and 77 (average 64.7). Higher CIA values may indicate more intense chemical weathering in more humid conditions or weathering in a sub-humid condition, whereas lower CIA values ca be attributed to an influx of less weathered detritus under semi-arid conditions.

The studied sediments were plotted on the A-CN-K (Al_2O_3-(CaO+Na_2O)-K_2O) diagram (Fig. 7c). The samples are arranged

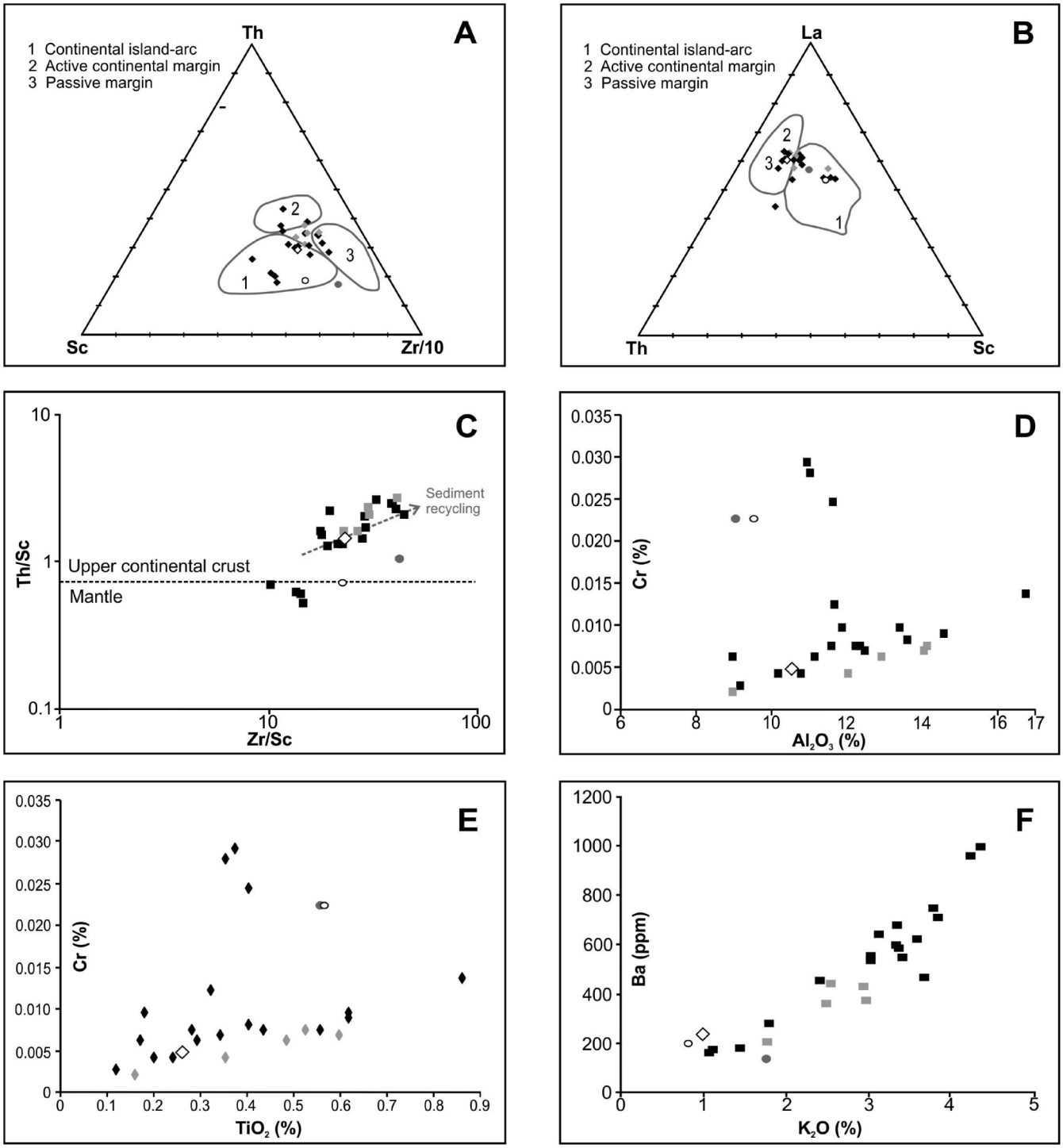

Figure 8: Discrimination plots of trace element geochemistry. A) Th-Zr/10-Sc ternary diagram, B) La-Th-Sc ternary diagram, C) Th/Sc vs. Zr/Sc, D) Cr vs. Al_2O_3, E) Cr vs. TiO_2, F) Ba vs. K_2O. For symbols for individual members of the ZF refer to Fig. 7.

almost parallel to the A-CN axis and follow a trend of increasing Al_2O_3 (and slightly also K_2O) with decreasing $CaO+Na_2O$. The elongated distribution reflects the varied role of the weathering trend/clay minerals and can be associated with grain size variations (Corcoran, 2005). Such a distribution indicates a prevailed physical weathering and the low influence of chemical weathering. Some subhorizontal distribution of the samples can possibly be interpreted as a result of a metasomatic increase in K during diagenesis (Fedo et al., 1995; Ohta, 2008). Alternatively, these patterns may indicate the mixing of a moderately weathered source with an unweathered one (McLennan et al., 1993).

With no extra input of detritus the sediment recycling results in a negative correlation of SiO_2 and TiO_2 (Gu et al., 2002) and also SiO_2 and Al_2O_3, Fe_2O_3, K_2O, MnO, and MgO are reflecting the quartz dilution effect. Such a trend can be generally followed for the samples. Whereas in the ideal case (Cox and Lowe, 1995; Corcoran, 2005) the overlying sequence should contain more quartz (i.e. SiO_2), less feldspar and clays (i.e. TiO_2, Al_2O_3, and MgO) the distribution is more complex in the studied cases (Fig. 7d). This can be connected with several factors: a) variations in fluvial discharge when a higher energy fluvial environment inhibited the removal of finer-grained feldspar, clay and heavy minerals richer in TiO_2 relatively to SiO_2; or b) by uplift and erosion of the source area during the all depositional history resulting in deposition of the stronger weathered portion first (Youngson et al., 1998).

The SiO_2/Al_2O_3 and Na_2O/K_2O ratios are highly susceptible to the effect of hydraulic sorting and grain-size fractionation (Ohta, 2008). On the SiO_2/Al_2O_3 - Na_2O/K_2O diagram (Fig. 7e) two compositional trends can be observed. Some samples are arranged horizontally and derived from the quartz-rich recycled sedimentary provenance. Obliquely arranged samples reveal an increased content of the material derived from the crystalline/igneous provenances.

The studied sandstones can be classified as lithic arenites or arkoses, only a few of them as wackes according to the diagram of Herron (1988) (Fig. 7f).

In terms of tectonic setting (Fig. 7g), the studied samples plot in the majority in the active continental margin field, while a number of them are in the passive margin (Roser and Korsch, 1988). Such an interpretation of the tectonic settings can be affected by the mobility of K and Na, particularly during the weathering of feldspar. The major element composition of studied samples is presented in Tab. 4.

4.4 Trace element geochemistry

In order to determine the tectonic setting, the samples were plotted on Th-Zr/10-Sc and La-Th-Sc ternary diagram (Bhatia and Crook, 1986; Fig. 8a, b). The samples are located in the

Sample	(ppm)										
	Ni	Th	Sc	La	Rb	Nb	Zr	V	Ba	Be	Co
ZP 1	18.6	8.00	4	20.3	131.5	4.6	112.7	19	708	1	3.3
ZP 2	45.4	17.50	8	20.2	113.4	8.1	154.4	36	676	1	7.7
ZP 3	34.8	7.80	6	21.8	108.6	6.2	132.8	30	635	0.5	5.1
ZP 4	28.8	14.50	9	31.9	134.8	11.0	202.7	53	370	2	8.8
ZP 5	34.3	5.60	4	14.6	120.0	3.5	110.5	13	994	0.5	4.3
ZP 6	74.1	12.90	8	24.1	98.9	9.6	138.6	44	533	2	9.4
ZP 7	117.8	7.30	7	18.9	61.2	10.6	288.4	41	134	0.5	10.8
ZP 8	103.2	5.70	8	16.2	28.5	10.3	177.6	38	192	0.5	12.3
ZP 9	30.2	7.50	5	21.3	136.4	6.1	88.4	35	957	1	4.4
ZP 10	42.5	13.50	6	30.3	144.0	8.4	239.7	38	741	2	6.2
ZP 11	12.7	10.50	4	19.6	134.2	5.6	128.4	25	465	0.5	2.9
ZP 12	14.9	4.90	2	10.4	62.0	3.8	76.6	15	277	0.5	2.4
ZP 13	105.6	5.50	9	19.5	44.9	8.1	119.0	55	155	1	10.3
ZP 14	114.2	5.30	9	17.0	46.8	7.4	126.2	56	167	1	11.3
ZP 15	112.7	6.90	10	19.4	61.0	9.1	100.0	60	177	0.5	17.4
ZP 16	7.5	0.41	3	14.2	116.6	4.2	89.3	16	358	4	2.3
ZP 17	52.7	0.89	12	21.2	119.1	14.6	171.3	47	581	7	8.5
ZP 18	36.4	0.69	6	30.9	121.4	9.3	262.2	32	544	2	5.4
ZP 19	37.6	0.53	5	19.7	47.2	5.6	113.0	24	234	4	6.9
ZP 20	144.4	1.18	16	51.8	117.0	16.7	302.2	90	552	4	14.9
ZP 21	26.0	0.79	8	33.7	94.1	10.3	209.7	44	200	4	7.1
ZP 22	79.5	1.06	10	40.8	92.5	12.1	284.5	65	448	2	11.2
ZP 23	72.7	1.10	9	54.1	153.7	15.4	343.2	52	617	2	12.9
ZP 24	31.3	1.28	9	50.1	129.0	14.3	363.7	55	425	2	9.6
ZP 25	21.9	0.90	6	30.2	107.3	8.4	176.1	41	439	2	6.4
ZP 26	19.0	0.29	3	10.6	123.8	3.1	63.3	16	594	<1	3.3

Table 5: The trace element composition (ppm) of studied samples.

fields of continental volcanic arc and continental margin (McLennan et al., 1993; Bhatia and Crook, 1986; Bahlburg, 1998).

The Th/Sc ratios vary between 0.52 and 2.63 (average 1.55), which point to variations in the content of felsitic and mafic rocks in the source area (Zimmermann and Bahlburg, 2003). The Zr/Sc ratios vary between 10.00 and 43.7 (average 25.56) The samples show the Th/Sc and Zr/Sc values (Fig. 8c) along the trend from the mantle to the upper continental crust composition (McLennan et al., 1993), the predominant provenance from the upper continental crust, a highly varied role of reworking and significant compositional heterogeneity in the source areas.

The average Cr content of the upper continental crust (UCC) is 83 ppm (Zimmermann and Bahlburg, 2003). The Cr values vary from 20.5 to 294.2 ppm. The elevated content of Cr (Cr above 150 ppm) was determined only in 17.5% of the samples. Samples from the upper parts of the stratigraphic successions reveal a generally lower content of Cr. An input from the mafic sources would also result in an enrichment of Ni and V. The abundances of Ni of the studied formations vary from 18.6 to 144.4 ppm (average 58.6 ppm). The V values vary from 13 to 90 ppm. Elevated abundances of Ni (i.e. Ni over 100 ppm) and the highest abundances of V were determined for samples from the Kalterbachgraben Sandstone/Siltstone Mb. and Rockenbauer Sandstone Mb. The Cr/Ni ratio is 0.9-3.23. The elevated Cr and Ni abundances with low Cr/Ni ratios (between 1.3-1.5) were suggested as having been indicative of source from mafic/ultramafic rocks (Bock et al., 1998; Sensarma et al., 2008). Low Cr/Ni ratios were recognised only in one sample from the Heiligenstein Arkose Mb. These results and also the low Y/Ni ratios (between 0.2 and 1.6) point to the limited significance of a mafic and ultramafic contribution to these deposits (McLennan et al., 1993).

Relative immobile trace elements like Cr, Ni and the major oxides Al_2O_3 and TiO_2 are thought to undergo the least fractionation during sedimentary processes (Sensarma et al., 2008). The relatively good correlation and different trends exist between Al_2O_3 and TiO_2 with Cr (Fig. 8d, e). The samples from the Kalterbachgraben Sandstone/Siltstone Mb. and Rockenbauer Sandstone Mb. reveal slightly different positions.

The immobile Ba shows a particularly strong positive correlation with K_2O (Fig. 8f), which can be connected with variations in the catchment area or variations in fluvial discharge (fluvial channel vs. crevasse channel).

According to Garver et al. (1996) Cr/Ba and Ni/Ba ratios appear to reflect the contribution from (ultra)mafic sources. In this context, Ba is thought to monitor the contribution of felsic crystalline rocks, an assumption that is supported by a positive correlation between feldspar and Ba contents of the sandstones. This discrepancy points to contrasting sources for Cr and Ni in at least some samples.

The Zr/Th ratio, which is another measure of the degree of recycling, varies from 8.8 to 39.5. An enriched value (above the UCC) was recognised in 28% of the samples. It results from

Facies symbol	Description	Interpretation
Fine-grained lithofacies		
Ml	Dark grey planar laminated clayey mudstone with rare laminas or thin flat lenses of very fine sandstone and siltstone. Sandstone laminas are discontinuous and disappear on the distance of several dm. Lenses are max. 2 cm thick. Occurrences of plant remnants and light mica. Beds are maximally 20 cm thick (most common thickness is only of several cm). Sharp planar base and sharp flat (often erosive) or convex up top of the beds. Commonly preserved only as an erosional relic within the beds of sandstone facies rarely in conglomeratic ones. Bioturbation is rare and restricted.	Deposition of waning stage flood in overbank areas (relatively distant to the distributive channels) (Hjellbakk, 1997), majority of deposition occurring from suspension settling and only limited bedload transport (weak currents). Plant development and preservation - either due to suitable climatic and/or non-oxidising conditions. Deposition also over the upper parts of sandstone or conglomerate beds – low relief flood plains.
Ms	Dark grey planar laminated clayey mudstone with common laminas and lenses of very fine, fine or medium sandstone. Sandy interbeds are discontinuous, maximally 7 cm thick and disappear on the distance of several dm. Ripple cross lamination in the thicker sandy interbeds. Occurrences of plant debris and light mica. Sharp planar or slightly concave base and sharp flat (often erosive) or convex up top of the beds. Often preserved only as an erosional relic within the beds of sandstone facies.	Alternation of suspension fallout and weak traction (low flow regime; waning flow conditions). Deposition in overbank areas (relatively proximal to the distributive channels) (Hjellbakk, 1997). Suitable climatic and/or non-oxidising conditions for plant preservation. Deposition also over the upper parts of sandstone or conglomerate beds - low relief flood plains.
Mm	Dark grey massive clayey mudstone. Occurrence of light mica. Preserved as an erosional relic within the beds of sandstone facies. Irregular shape with thickness of maximally 20 cm and maximal lateral extent of 2 m, sharp flat to slightly irregular base, flat erosive top.	Rapid fallout from overbank flood; oxidation after deposition (Walker and James, 1992). Deposition also over the upper parts of sandstone beds - low relief flood plains.

Table 6: Lithofacies recognised within studied outcrops and their brief description.

Facies symbol	Description	Interpretation
Sandstone lithofacies		
Sl	Light reddish brown, brown, grey-brown, grey, very fine to fine, medium, rarely coarse grained, planar to low angle laminated sandstone. Often relatively well sorted. Occurrences of plant debris in some outcrops (some fragments about 10 cm large) and light mica. Thickness of individual sets about 10 cm, locally vertically aggraded into cosets about 0.3-1 m thick. Locally fining upward trend. Base sharp erosive (in FA1), commonly with mud flasers or mud chips (sometimes even 3 cm large) along the base (especially if Sl is superimposed over mudstone facies). In the case of FA2 facies preserved as erosive relics within conglomeratic beds with scattered isolated subrounded pebbles up to 2 cm. Tabular, lensoidal to broadly channelized shape, sharp planar, irregular or concave base, sharp flat top of the beds.	Upper flow regime stratification, very flat dune migration, (Smith, 1974). Suspension settling and traction; bursting of turbulent boundary layers (Bridge, 1993; Cheel and Middleton, 1986). Migration of small-scale 3D bar and/or planebed macroforms; deposition on sloped surface; migration in shallow water.
Sr	Light grey, brown-grey to green-grey ripple cross laminated, very fine to fine sandstone, relatively well sorted. Usually irregular (broad channel) beds with concave base and sharp flat (sometimes erosive) top. Individual sets are usually about 6-15 cm thick. The basal portion of thicker sets could reveal planar parallel lamination. Local occurrence of several mm thick mudstone flasers or max. 2 cm thick erosive remnants of facies Ml within thicker packages of facies Sr. Content of small (mm large fragments) plant debris varies.	Sedimentation during migration of current / asymmetric ripples, lower flow regime conditions, thicker sets with planar lamination in the lower part point to periods of rapid sediment accumulation from waning flows, filling of smaller crevasses.
Sp	Brown to light brown, coarse to medium grained, rarely fine grained, planar cross stratified sandstone, mostly poorly but in some cases well sorted, with admixture of light mica. Beds have broadly channel shape, scoured concave base and flat almost planar or convex up top. Beds can be laterally followed on the distance of 5 m. Thickness of sets 8-12 cm, cosets max. 60 cm. Commonly fining upwards trend in sets. Sometimes scattered subrounded pebbles up to 1.5 cm (in the case of FA2) or mud flasers (in the case of FA1) along the reactivation surfaces.	Migration of 2D fluvial dunes, avalanching along bar / dune margins (Harms et al., 1975), filling of the channels (both fluvial and crevasse channels). Accretion, aggradation.
St	Grey, brown-grey, brown, fine to very fine, medium to coarse, rarely very coarse grained, trough cross stratified sandstone. Low angle of the dip. Individual sets up to 10 cm thick, cosets about 30-60 cm thick. Beds have broadly channel shape, sharp erosive concave base, flat almost planar or convex up top, rarely erosive shape. Sometimes (superposition of mudstones facies) occurrence of mud chips (5 cm) or mud flasers (up to 5 mm thick) along the amalgamation surfaces. Varied occurrence of angular to subangular scattered pebbles up to 3 cm, very exceptionally cobbles (22 cm in A-axis). Pebbles mostly along the base, locally occurrence of discontinuous "pebble strings".	Migration of 3D dunes in shallow water (Harms et al., 1975), filling of the channels or scour fills, traction processes during lower flow regime conditions. Accretion, aggradation.
Sm	Brown to light brown fine, medium to coarse grained massive sandstone, admixture of angular to subangular granules and pebbles up to 3 cm, light mica. Concave base, concave top.	Rapid suspension fallout from highly concentrated flows (Smith, 1974). Sediment gravity flow; near-surface currents.
Sg	Brown, coarse to very coarse, gravelly sandstone, higher content of granules and subrounded and subangular pebbles (up to 3 cm), poorly sorted, massive or crude low angle planar stratification. Pebbles especially along the base, elongated pebbles are preferably oriented parallel to bedding plane (A p). Sharp, flat, often erosive base and sharp top. Multiply amalgamated beds, set thickness 5-10 cm. Sometimes preserved as erosive relic within the conglomerates. Beds laterally traceable on the distance of max. 5 m.	Rapid deposition under waning stage in alluvial channel or sheet floods (Blair and McPherson, 1994); bedload pulsation (Reid and Frostick, 1987).

Table 6 continued

the low values of both Th and Zr, especially from the lower Th concentrations. Th is commonly abundant in heavy minerals like monazite, zircon, titanite, the minerals of the epidote group, and clay minerals. The results point to different provenance and the lower role of recycling since the concentrations of the heavy minerals during recycling would accordingly lead to an increase in Zr and Th abundances in the respective deposits (Zimmermann and Bahlburg, 2003). Variable enrichment in Zr compared to the UCC (190 ppm) probably reflects an increased influence of hydraulic selection and/or sedimentary recycling. The trace element composition of studied samples is presented in Tab. 5.

Facies symbol	Description	Interpretation
Conglomerate lithofacies		
Gm	Clast-supported conglomerate, disorganised, subangular to rounded pebbles. Thickness of sets about 10 cm, multiply amalgamated, cosets up to 50 cm thick. Broad concave, commonly erosive base, clasts along the base usually about 7-15 cm, with outsized boulders up to 55 cm. Sometimes fining upward trend in bed. Locally preserved only as pebble lag.	Flood deposits, channel infill (Maizels, 1989, 1993; Todd, 1989).
Gh	Clast- to matrix supported conglomerate, grading upwards into coarse to very coarse sandstones with granules as scattered pebbles. Massive, sometime planar to low angle inclined lamination in the topmost parts of the beds. Flat, concave upward base with outsized cobbles (up to 15 cm), rarely outsized clasts along the top. Pebbles and cobbles rounded to subrounded, usually about 2 cm. Matrix formed by coarse to very coarse sandstone with granules. Individual sets 20-50 cm thick, cosets up to 65 cm thick.	Poor sorting, polymodal clast distribution and absence of stratification and chaotic fabric suggest rapid deposition by hyperconcentrated flood during catastrophic flood event and/or heavy rainfall.
Gms	Matrix supported conglomerate, matrix formed by coarse to very coarse sandstone and granules. Mostly disorganised, ungraded, rarely crude horizontal stratification and coarse tail inverse grading. Clast size varies between granule and cobble size (max. about 65 cm) with a dominance of medium to coarse, rounded to subrounded pebbles. Outsized clasts commonly along the base of the beds, rarely also close to the top. Locally pebble clusters. Bed thickness varies between 10-50 cm. Common amalgamation of beds. Irregular flat, horizontal or inclined base, both erosive and nonerosive.	Cohesionless debris flow deposits (Bull, 1997; Larsen and Steel, 1978).
Gl	Clast to matrix supported pebbly conglomerate to gravellite with scattered pebbles, low angle planar stratification. Subangular or subrounded pebbles mostly about 3-5 cm (A-axis). Elongated pebbles with preferred orientation (A p). The beds reveal the shape of flat channels with concave, commonly erosive base and flat top. Outsized cobbles up to 26 cm along the base common, rarely also along the top. Thickness of sets about 10 cm, cosets 30-200 cm thick. Commonly variations in the grain-size and pebble content in the adjacent sets.	Stratification and preferred clast fabric suggest deposition by stream flows (bed load transport), waning flow deposition by accretion, vertical accretion and downstream migration of low relief bedforms or gravel and sand sheets (Jo and Chough, 2001; Brayshaw, 1984).
Gt	Very coarse grained sandstone, gravellite or pebble conglomerate, trough cross stratified, commonly low angle of the dip. Isolated large pebbles to very rare cobbles (max. 30 cm A-axis) along the base relative common, rarely recognised along the top. Subrounded to rounded pebbles mostly up to 4-10 cm. FU trend in the thicker beds. Openwork to clast supported, rarely (mostly upper part of the beds) matrix supported (sand matrix). Preferred orientation of the elongate clasts (both A p and A t). Beds have sharp erosional bases. Individual sets are 10-30 cm thick, cosets are usually 50-70 cm thick.	Low angle cross-stratification, scouring basal contact point to lateral accretion and slip face deposit on longitudinal bar or hollow infill.

Table 6 continued

4.5 Interpretation of the provenance analyse data

The predominance of quartz as well as certain amounts of plagioclase and alkali feldspar reflects the derivation from the granitic rocks. Polycrystalline quartz grains, presence of muscovite and the deformation features suggest mica schists as source and metamorphism exceeding greenschist facies. According to Einsele (1992) the preservation and transport of feldspar, particularly of less stable plagioclase, is an indicator of limited chemical weathering condition.

The significant presence of garnet and the occurrence of staurolite mainly indicate mica schist complexes as primary sources. The monotonous spectra of the garnet composition indicate a primary source and the predominant provenance from gneisses, (amphibole+biotite) schists and granulites. ZTR minerals are common in acidic to intermediate magmatic rocks as well as in mature siliciclastic sediments and certain metamorphic rocks (Eynatten and Gaupp, 1999). Moreover, high ZTR values might also point to extensive diagenetic dissolution of less stable minerals (Garzanti and Andò, 2007). The predominant source of rutile were metapelitic rocks (mica schists, paragneisses, felsitic granulites). Approximately 14.1% of the rutiles originate from metamafic rocks (eclogites, mafic granulites) and approximately 21% of the studied rutiles in all probability from magmatic rocks. Approximately 2.4% resp. 4.4% of the rutile could not be discriminated in relation to the source rocks. Apatite may be derived from biotite-rich rocks but is a common accessory mineral in almost all igneous and a number of metamorphic rocks (Adhikari and Wagreich, 2011). Epidote was derived from the low-grade metamorphic series. Kyanite indicates the presence of high-pressure metamorphic rocks. The presence of andalusite also reveals the provenance from a higher-T metamorphic facies. Spinels indicate the existence of basic/ultrabasic rocks in the source area.

Zircon points to an important role of magmatic rocks in the source area. Niedermayr (1967) has documented the elongation of zircons for the Gföhl gneiss between 1.8 and 2.3 and for the granulites of St. Leonhard between 1.5 and 1.7. Hoppe (1966) has revealed the elongation in the granulites of St. Leonhard of about 2.

The Moldanubian unit was the predominant source area for the ZF. Today Moldanubian rocks crop out mainly west of the ZF but they are also present east of the ZF. The Moldanubian rocks east of the ZF are displaced by the Diendorf fault system and it is doubtful, if this already was the case in the Late Palaeozoic.

Despite limited amount of the analyses, we can only speculate as to the general evolution in the source area. A local source from weathered crystalline rocks can be assumed for the basal successions. A wider provenance, less weathered detritus, the predominance of mica schist complexes and the minor role of reworking and floodplain modifications can be assumed for additional, younger parts of the succession. The results do not indicate the successive exhumation of a simple structured (lower- to higher grade metamorphic source) orogen but may be interpreted as differences in expansion in the source areas. The source areas seem to be largely stable during the depositional history and derivation is supposed from mainly primary sources.

The studied sandstones are poorly sorted and reveal a relatively immature composition implying a short transport distance and rapid deposition. The higher proportion of unstable lithic components and the moderately high feldspar content indicate a high-relief source area. The prevailing physical weathering and the low role of chemical weathering can be confirmed by geochemistry. Sediments will be least affected by the chemical weathering in tectonically active areas where rapid uplift not only maintains steep slopes but also continually brings a fresh supply of unweathered bedrock. Wide fluctuations of mineral percentages and indices indicate local sources, which is in accordance with the interpreted depositional environments, and are regarded as typical for post-orogenic sedimentary basin fills such as the extensional collapse grabens. They can also reflect the hydraulic conditions during deposition (Morton, 1985).

The role of climatic variations in the affection of a heavy mineral suite is probable. Significantly lower contents of apatite were determined in the Stephanian deposits compared to Autunian deposits. A lack of apatite in the source rocks is not probable, as apatite is a common mineral in metamorphic or igneous rocks and apatite is relative resistant to burial processes. Wide variations in the ATi ratios suggest that the ratio are likely to be, at least in part, a function of weathering during alluvial storage (dissolved by contact with acidic waters)

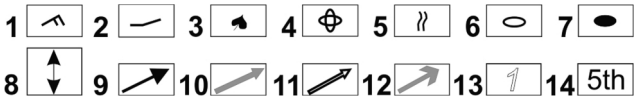

Figure 9: Schematic lithostratigraphic logs with lithofacies distribution of selected outcrops of the ZF. For position of the outcrops 9A - 9I refer to Table 1 and Fig. 1. Explanation to the symbols: 1: ripple cross lamination, 2: erosional remnant of mudstone bed, 3: remnants of plant stems, 4: concretions, 5: bioturbation, 6: outsized clasts, 7: mudstone intraclasts, 8: crevasse channel, 9: channel axis, 10: accretional surfaces, 11: cross-stratification foresets, 12: elongated clasts, 13: types of multi-storey crevasse channels, 14: order of the bounding surface according to Miall (1996).

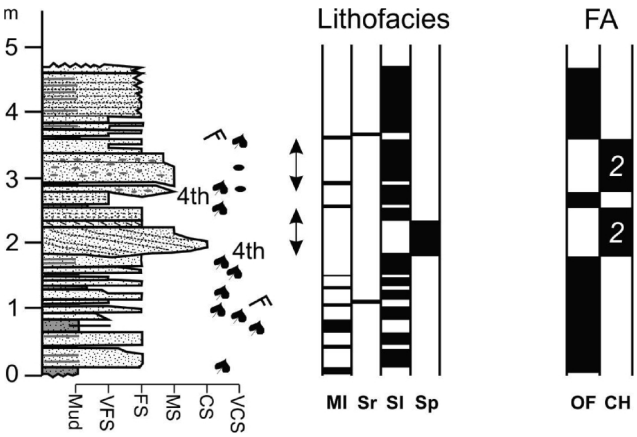

Figure 9A: Outcrop 1 (Rockenbauer Sandstone Mb.).

(Morton and Hallsworth, 1999; Hallsworth and Chisholm, 2008; Adhikari and Wagreich, 2011). Possible burial of deposits below 3.5 km calls into question the validity of GZi, ATi and MZi indices.

There are two reasonable possibilities for the differences in the heavy mineral assemblages connected with higher content of rutile, zircon and apatite in some samples, where garnet usually dominates. These possibilities are: 1) a sudden delivery of these minerals connected with processes in the source area (variations in the source rocks, sediment recycling, cannibalization of the older basin infill – especially Rockenbauer Sandstone Mb.), 2) consequence of complex hydraulic processes when different hydraulic behaviour of individual heavy minerals distorted the provenance signals (Morton and Hallsworth, 1999; Cascalho and Fradique, 2007).

4.6 Facies analyses and depositional environment

4.6.1 Facies analysis

Individual lithofacies were selected according to grain-size, internal organisation, stratification, colour, and bedding geometry. They are briefly described in Tab. 6, their occurrence on individual outcrops can be followed in Fig. 9a-9i, and examples are presented in Fig. 10a-10h and Fig. 11a-11d. Lithofacies can be grouped into gravel, sand and mud categories based on the dominant grain-size. The occurrences of individual lithofacies and facies associations significantly differ in the lower part of the studied sedimentary succession of the Zöbing Formation.

In each case only one locality was available for the study of the Rockenbauer Sandstone Mb. (Fig. 9a) and the Kampbrücke Siltstone Mb. (Fig. 9c) whereas two outcrops were logged for the Kalterbachgraben Sandstone/Siltstone Mb. (Fig. 9b, 9i). Nine lithofacies (Ml, Ms, Mm, Sr, Sp, St, Sl, Gt, and Gm) were recognised. The most common are the fine-grained facies, whereas the conglomeratic ones are very rare.

Fifteen localities were studied in the Heiligenstein Arkose Mb. (Fig. 9d-9h) and 14 lithofacies were identified in the outcrops. Although the conglomeratic lithofacies usually dominates, the presence of sandstone lithofacies is sometimes remarkable. The occurrence of fine-grained facies is very variable: it can be absent, represent a subordinate portion, or exceptionally it can have volumetric importance.

Only one locality was available for the study of the Geißberg Sandstone Mb. In this locality 5 lithofacies were recognised: Mm 2.4%, Sr 36.6%, Sl 6.1%, Sm 6.1%, and Gms 48.8%.

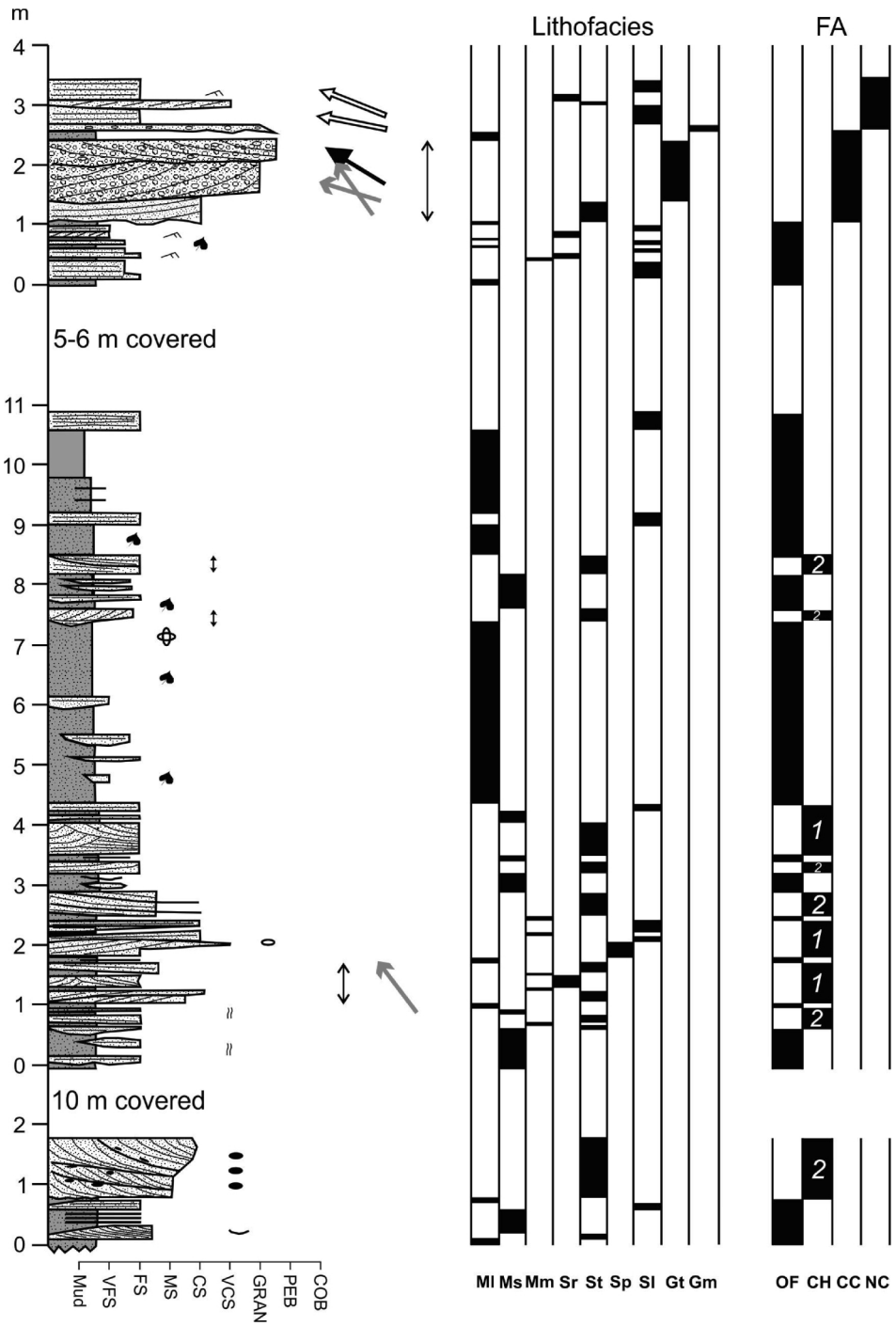

Figure 9B: Outcrop 2 (Kalterbachgraben Sandstone/Siltstone Mb.).

All three studied localities of the Lamm Siltstone/Arkose Mb. were small and the rocks strongly tectonised. Seven lithofacies were recognised within the deposits of this member (Ml, Sl, Sg, Ml, Gl, Gh, and Gms).

4.6.2 Facies associations and architectural elements

A facies association is defined as an assemblage of spatially and genetically related facies representing a particular morphodynamic style of sedimentation, involving specific facies, bed geometries and depositional architecture (Miall, 1989; Nemec, 2005). The recognised lithofacies have been grouped into four lithofacies associations: i.e. (a) non-channelized fine-grained deposits (OF), (b) channelized sandstones (CH), (c) non-channelized conglomerates (NC), and (d) channelized conglomerates (CC). The facies associations within the alluvial setting are commonly described also as architectural elements. More detailed division into sub-associations was possible in some case.

4.6.2.1 Non-channelized fine-grained deposits (OF)

Non-channelized fine-grained deposits (OF) typically form tabular bodies (normally with a broadly planar base and erosive top) of the dominant mudstones interbedded with up to decimetre-scale flat beds of siltstones and fine-grained sandstones. Two sub-associations can be distinguished within these deposits. The first one is formed by up to 3 m thick beds of the facies Ml and Ms with thin (a few cm thick) intercalations of facies Sl and rarely Sr. Thicker (a few dm thick) tabular sandstone beds of Sl facies encased within mudstones are characteristic for the second subassociation. OF dominate within the

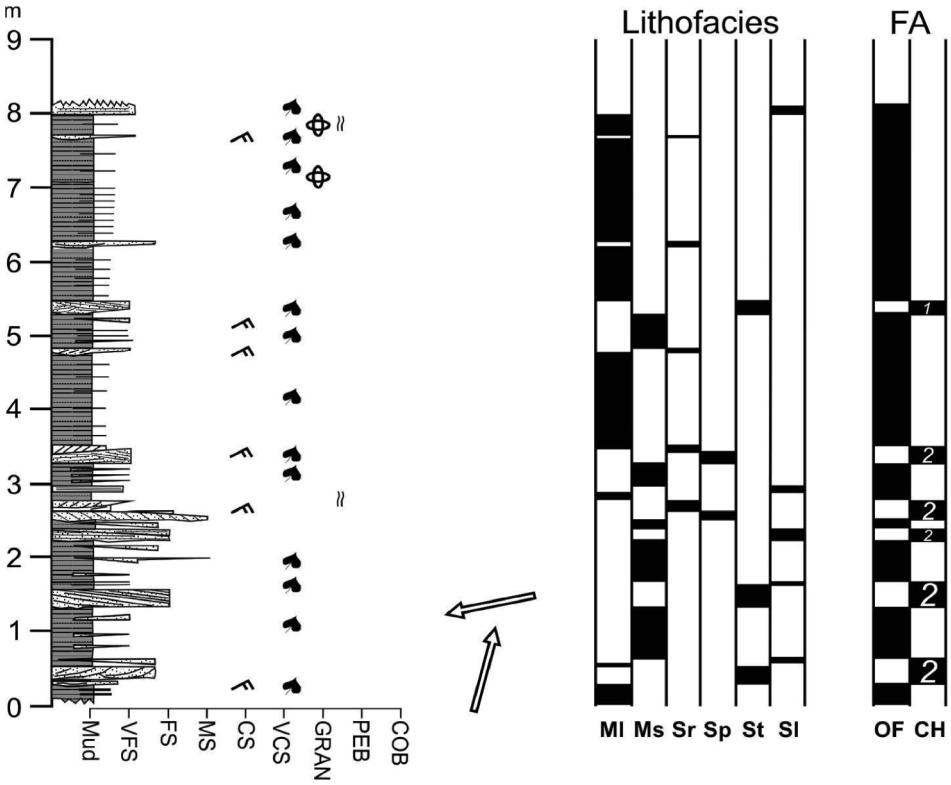

Figure 9C: Outcrop A (Kampbrücke Siltstone Mb.).

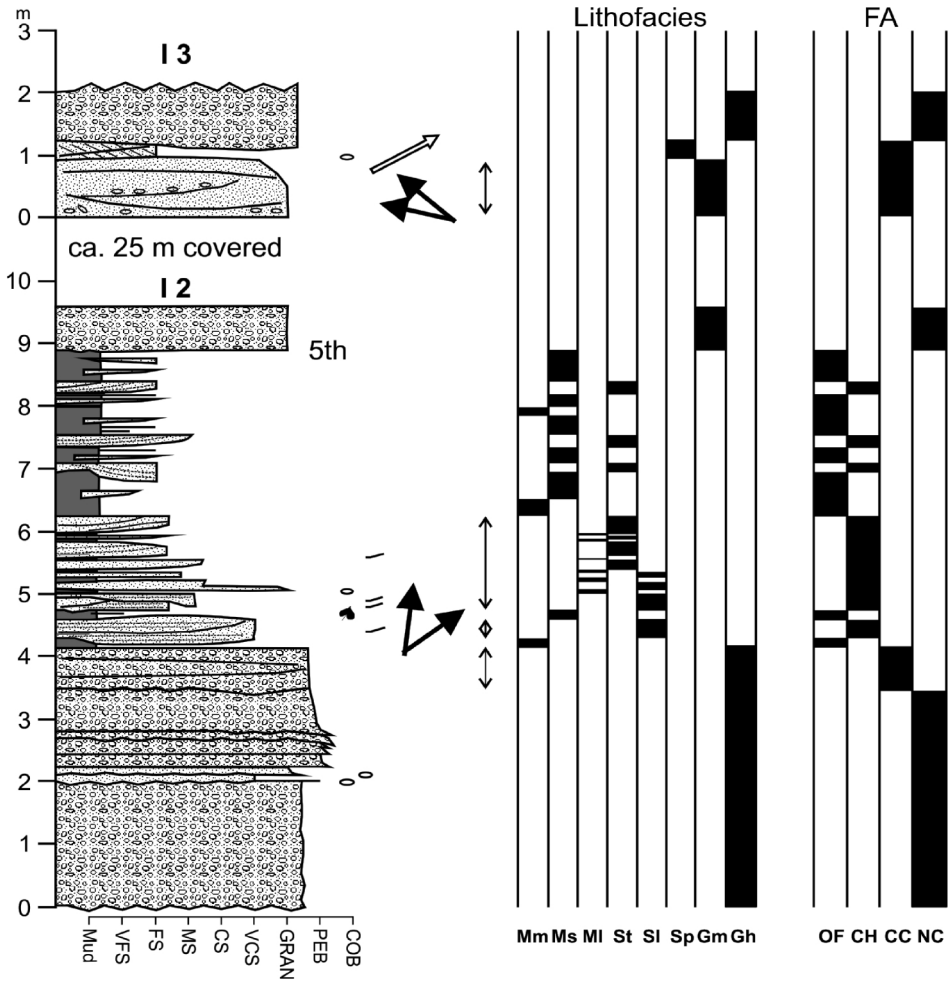

Figure 9D: Outcrops I2-I3 (Heiligenstein Arkose Mb.).

Rockenbauer Sandstone Mb., the Kalterbachgraben Sandstone/Siltstone Mb. and the Kampbrücke Siltstone Mb., forming between 58.6% and 81.3% of the successions, where they were deposited in a succession with channelized sandstones. These deposits were recognised rarely within the Heiligenstein Arkose Mb., where they are mostly preserved as up to 10 cm thick discontinuous erosional relics (facies Mm) within channelized conglomerates or sandstones.

Interpretation: The OF are interpreted as floodplain deposits. A close association with channelized sandstones and conglomerates is indicative for such an environment. The first subassociation represents fine-grained floodplain deposits and the second one levees or crevasse splays. We can speculate about overbank deposition during and after floodplain inundation laterally associated with a fluvial/distributive channel or downslope terminal floodplain regions. Generally they can also be ascribed according to Miall (1985) as overbank fines (OF).

During high discharge events, the flow expanded over contemporaneous floodplains depositing sandstone facies Sl or Sr (López-Gómez et al., 2009; Turcq et al., 2002). Horizontally stratified and ripple cross-stratified sandstone may suggest oscillation between high-flow and low-flow conditions during a single depositional event. The predominance of tabular beds consisting of Sl or Sr lithofacies, suggests that flow events were short-lived, ephemeral and of high intensity (Tunbridge, 1981). Tabular sandstone beds could also represent deposition associated with unconfined flow just downslope of the confined channels (downslope terminal splays). However, the areal extent of the outcrops did not allow the identification of the transition from channelized to unconfined flow, or the distinction between levees or splays, or overbank crevasse splays and downslope terminal splays. Mudstone facies reflect deposition of waning stage flood or can represent a slightly distant part of the floodplain (in relation to channels).

Rare bioturbation (only in Ms and Ml facies) and the absence of pedogenic reworking are suggestive of relatively rapid deposition and short periods of relative sediment starvation. The thickness of the bedding and colour provide evidence of deposition under oxidation conditions in shallow to ephemeral water bodies and rapid burial. This is associated with a high water table and surface ponding that enabled the preservation of plant detritus.

4.6.2.2 Channelized sandstones (CH)

This facies association constitute typical channelized beds of dominant Sp, St or Sl facies, subordinate Sr facies and rare Ml facies. The channelized sandstones (CH) were described in the Rockenbauer Sandstone Mb., the Kalterbachgraben Sandstone/Siltstone Mb., the Kampbrücke Siltstone Mb., and the Heiligenstein Arkose Mb., where they form 9.5% to 32.6% of the succession, and were mostly identified in succession with OF. The channelized sandstones can be further subdivided according to their internal organisation into: a) single-channel fill ("storey"), which reveals lenticular geometry, b) complex channel fill ("multi-storey"), which is represented by multilateral complexes.

Single-storey channels are about 20 cm deep and filled with several sets of fine to very fine-grained sandstone of St facies.

Three types of infill were recognised within the multi-storey channels. The first one is formed by coarser-grained and thicker sets of Sp or St facies in the lower part of the channel, and thinner and finer-grained beds of Sl or Sr facies in the upper part. Individual sandy beds are often covered by thin mudstone interbeds. Irregular mudstone rip-up clasts are common, typically placed along the bases of beds of cross-stratified facies. The thickness of the channel infill ranges from 20 cm to 90 cm, a finning upward trend is typical. The deeper channels typically reveal coarser infill than the shallower ones, with a volumetrically predominant cross-stratified part. This type of multi-storey channel was recognised only in the Kampbrücke Siltstone Mb.

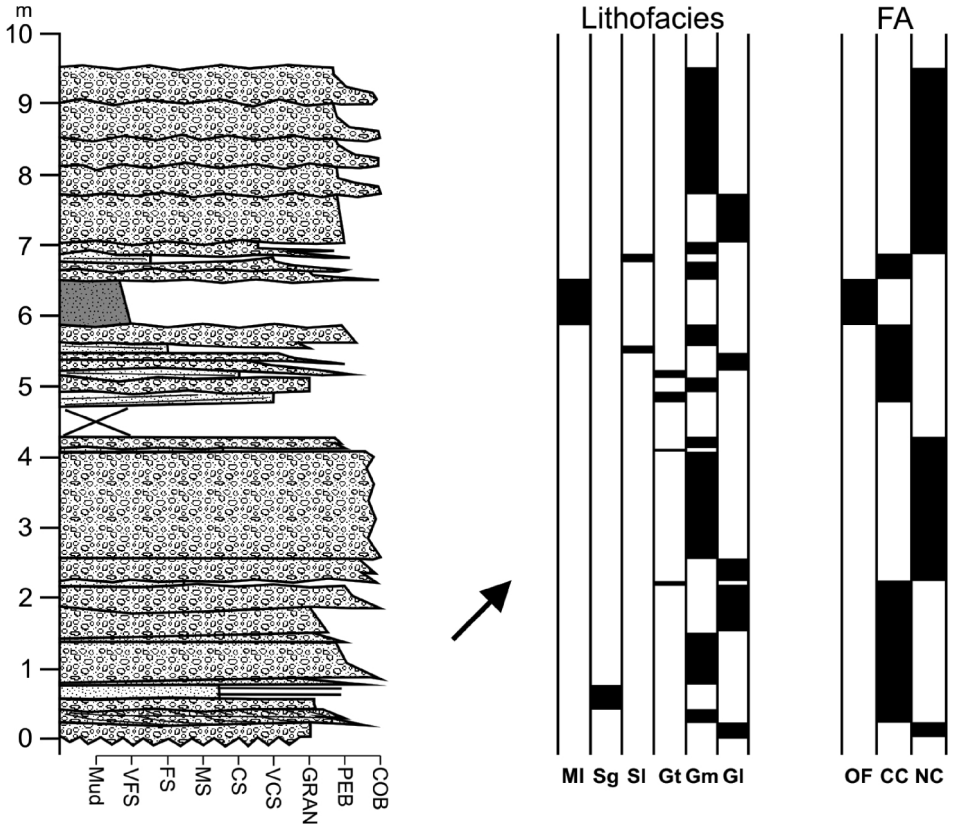

Figure 9E: Outcrop H (Heiligenstein Arkose Mb.).

The second type of multi-storey channel is formed only by sets of cross-stratified Sp or St facies, which are separated by thin interbeds of mudstone. Irregular mudstone rip-up clasts are typically scattered along the bases of sandstone beds. The thickness of the channel infill ranges from 20 cm to 100 cm in the Kampbrücke Siltstone Mb. Sets of coarser-grained sandstones of facies St, with scattered granules were recognised with this type of channel in the Heiligenstein Arkose Mb. The set thickness ranges from 10 cm to 25 cm and the channel width from about 1 to 1.5 m. However, commonly the channel width was beyond the extent of the outcrop.

The third type of channel infill is formed exclusively by Sl facies. Individual beds of Sl facies are separated by thin interbeds of Ml facies and irregular mudstone rip-up clasts are typically found around the bed bases. The thickness of the channel infill ranges from 15 cm to 80 cm. The deeper channels reveal a fining upward trend of infill, whereas the shallower ones are finer grained. Infill of this type of channel in the Heiligenstein Arkose Mb. is significantly coarser grained (compared to the Rockenbauer Sandstone Mb., the Kalterbachgraben Sandstone/Siltstone Mb., and the Kampbrücke Siltstone Mb.).

Interpretation: The CH have arisen via confined (in-channel) fluvial processes and are generally interpreted as crevasse channels. Single-storey channels are interpreted as mostly short-lived structures reflecting the erosion of the floodplain by a sudden high discharge event in which the channel scoured a single broad erosional surface. The multi-storey channels reflect several stages of filling/accretion (lower part) and aggradation (upper part). The concave erosive base, mudstone chips near the base and the cross-stratified packages of Sp or St facies suggest, that the lower part represents scouring and subsequent almost immediate filling. This cross-stratified part could be connected with lateral or downslope migration of dunes. The upper part would represent deposition on a plane or low-relief bed, reflecting rapid aggradation. Periods of peak discharge in channels were also responsible (perhaps partly) for flooding in overbank floodplain environments. Mud drapes along accretion surfaces imply that, in addition to recurring episodes of scour and fill during peak flood conditions, there were multiple episodes of suspension fallout during late-stage waning flood flow. The small thickness of sandstone beds can be connected to rapid deposition from shallow flows due to seasonal or ephemeral supply (Hampton and Horton, 2007). The differences in the geometry (especially thickness), grain-size of the infill and various types of infill of multi-storey channels can be explained by proximal distal variations. The deeper channels are presumed for the proximal part of the crevasses, predominantly filled with cross-

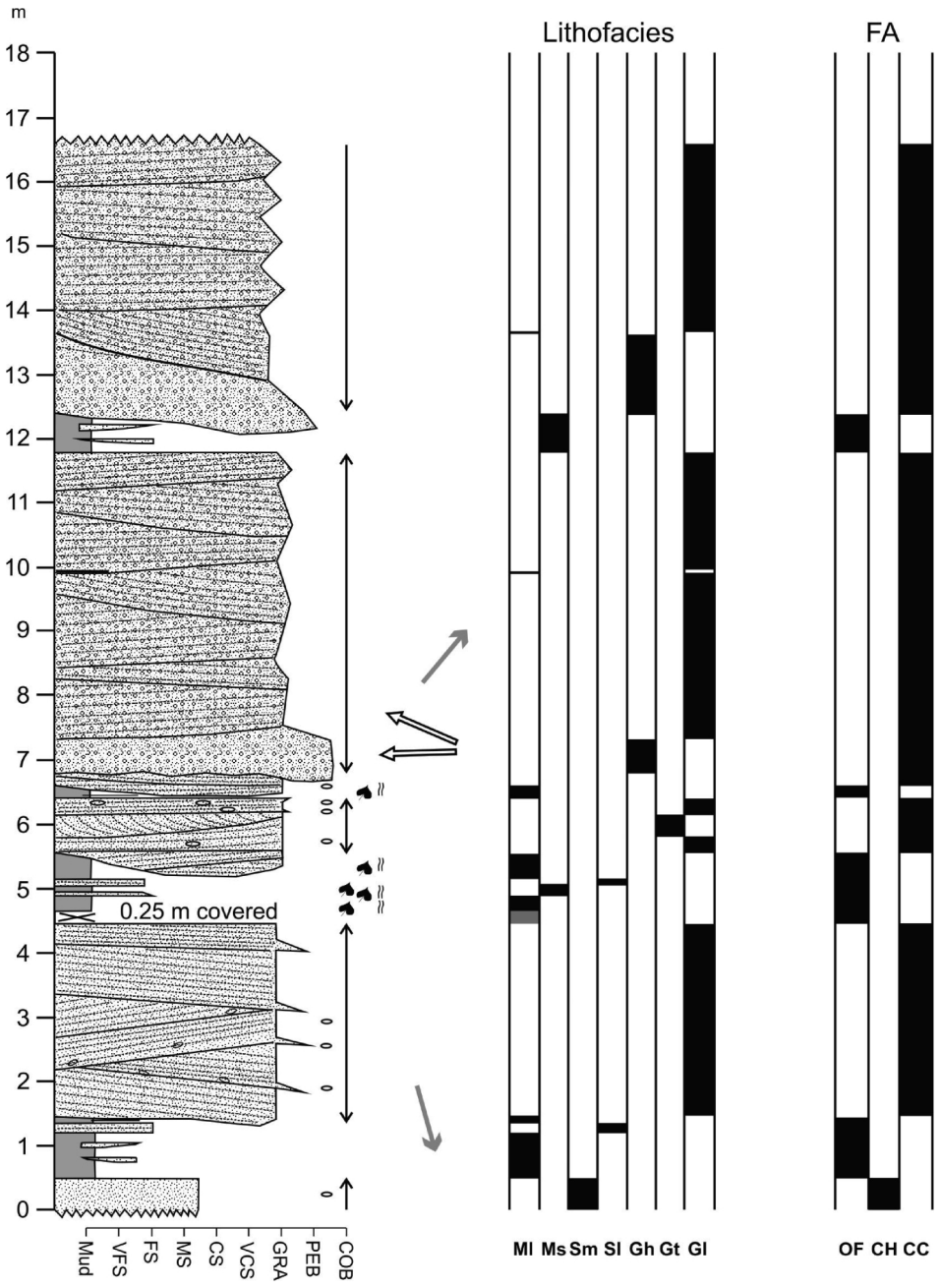

Figure 9F: Outcrop L (Heiligenstein Arkose Mb.).

stratified and coarser sandstones. They point to more sustained discharge and lateral or downslope migration of three-dimensional dunes. The shallow channels are connected with distal or terminal parts of the crevasses, typically filled with finer, thinner beds of Sl facies. The dominance of facies Sl is often explained by flash stream discharge common in dry-land river systems (Tunbridge, 1981; Sneh, 1983; Olsen, 1989; Fisher et al., 2007). The channels seem to be relatively stationary until completely filled by a single or multiple flood event, and only then avulsed to an adjacent part of the floodplain.

Deeper and thicker crevasse channels with a coarser-grained infill within the Heiligenstein Arkose Mb. could be connected with more proximal parts of the floodplain, or with the evolution of the complete depositional system.

4.6.2.3 Channelized conglomerates (CC)

This facies association is characterised by an erosive concave base and dominant conglomeratic infill. The lateral extent of the channels was larger than the outcrop scale. We can speculate about a width of more than 15 m in some outcrops. The broad flat channel floors locally display a stair-stepped profile. The channelized conglomerates (CC) represent the highly predominant part of the Heiligenstein Arkose Mb. They were also recognised in the Kalterbachgraben Sandstone/ Siltstone Mb., where they represent only 3% to 9.6% of the succession.

The CC were recognised either in association with OF or with non-channelized conglomerates (NC). The CC connected with OF have erosive base (incised into the fine-grained non-channelized deposits) and their thickness ranges from 0.5 m to 5.0 m. Erosive relics of interbeds of Ml facies within the channel infill and also flat channel top (covered by a tabular bed of Ml facies) were often recognised. The infill of the channel is complex. Irregular wedge shaped sets (thickness about 10-30 cm) of Gl or Gt facies without any grain size variation from the base to the top was recognised sometimes. The fining upward trend was also noticed, when sets of Gm, Gt, Gl or rarely Gh facies are superposed by sets of St, Sl or Sr facies. However, coarsening upward succession with medium to coarse-grained sandstone of St facies on the base, followed by conglomerates of Gt facies and common mudstone rip-up clasts was also observed.

The CC recognised in association with the NC seem to be smaller in scale of channels. We can speculate about a width of 4.0 m to 5.0 m and thickness ranges from 0.3 m to 1.0 m. An erosive top is typical. Complex infill with a general fining upward trend was often recognised. Sets of Gm, Gt or Gl facies were found in the lower portion of the channel. The upper portion is formed by Sr or Sl facies with bed thickness of 5 cm to 10 cm. Some channels were infilled only by coset of Gt or St facies (coset thickness ranges from 30 to 60 cm). The sandstone of such channels is often gravelly or with thin interbeds of Gm facies.

Interpretation: The CC reflect an origin from confined water/ stream flows and hyperconcentrated flows. Hyperconcentrated flow represents a subaerial, fluidal, turbulent flow of water-sediment mixture that is excessively dense and hence deposits sediment mainly or entirely in a non-tractional manner (Nemec, 2009). Their origin here is connected with the dilution of debris flows in stream channels (Nemec and Muszyński, 1982; Sohn et. al., 1999) reflecting a "transition" to stream flows. The CC are significantly thicker than the CH. We can speculate about relatively larger (deeper and wider) channels with the possibility of a longer existence. However, the relatively small thickness of the cross-stratified beds precludes deep channels. The close association between, both the NC

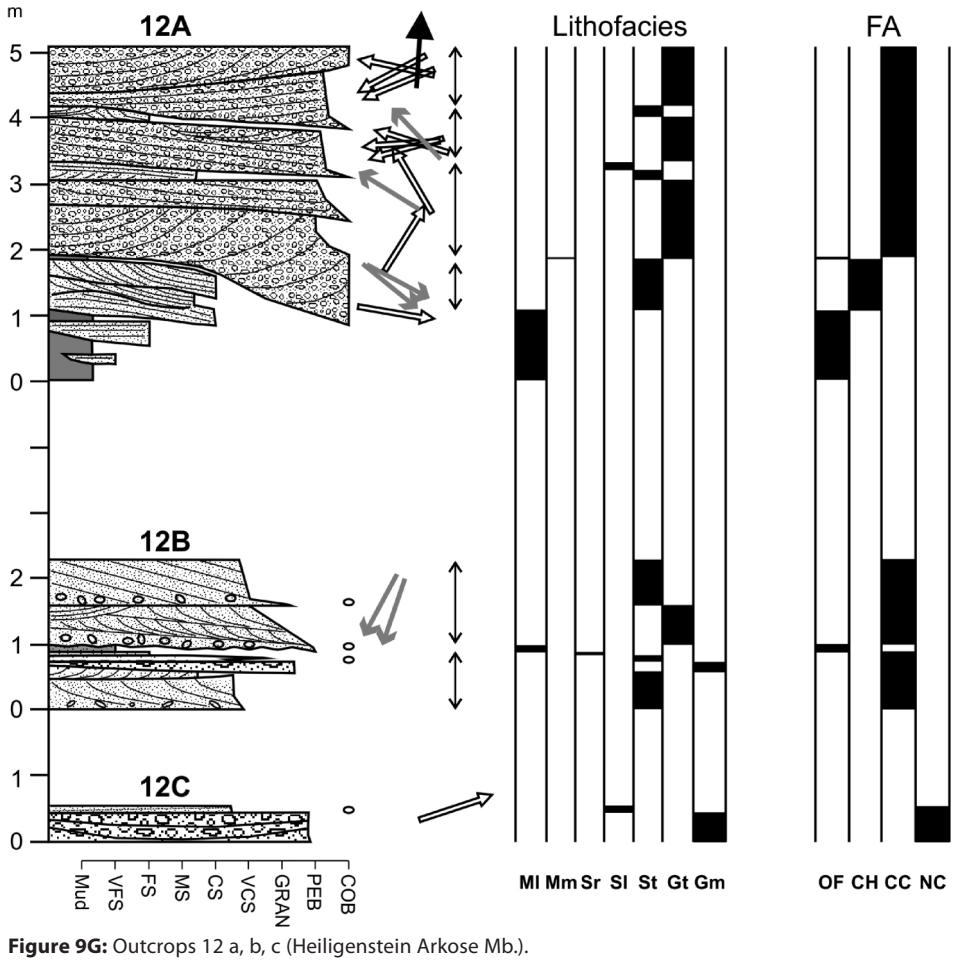

Figure 9G: Outcrops 12 a, b, c (Heiligenstein Arkose Mb.).

and the CC, and the OF points to accumulation associated with a coarse-grained fluvial system, or a fluvial fan accompanied (downslope/terminally?) by extended floodplain.

The complex infill and alternation of cross-stratified facies (Gt, St) with planar stratification (Gl, Sl) and massive ones (Gm, Gh) reflect variations in water discharge and discontinuities in the accretion of the beds (Nemec and Steel, 1984). Similarly, the reoccurring thin laminated and massive mudstone drapes of conglomerate beds and the stair-stepped profile of the channel base are evidence for variations in fluvial discharge, which could be connected to seasonality of precipitation and cyclicity of flood events (Mack et al., 2003). On the other hand, the fining upward trend of the channel infill in association with the lateral accretion of the beds points to more continuous infill of the channel and migration of the flow along the floodplain. Significant variations in the thickness of sets (especially Gt and Gl) reveal that the streams were relatively shallow. The occurrence of rippled sandstones along the upper most flat part of the channels may indicate deposition during the final phases of their abandonment. The dominance of water flow or water-rich mass flows (hyperconcentrated flows) and outwashed tops suggest the presence of wet-type fans and plains under semi-humid to semi-arid seasonal climates.

4.6.2.4 Non-channelized conglomerates (NC)

Non-channelized conglomerates (NC) did not reveal a clear channelized base of the beds (on the outcrop scale). The bases are horizontal or inclined, often sharp, planar and slightly uneven (cm scale relief). The presence of outsized clasts (even boulders to a max. of about 50 cm in diameter) along the base

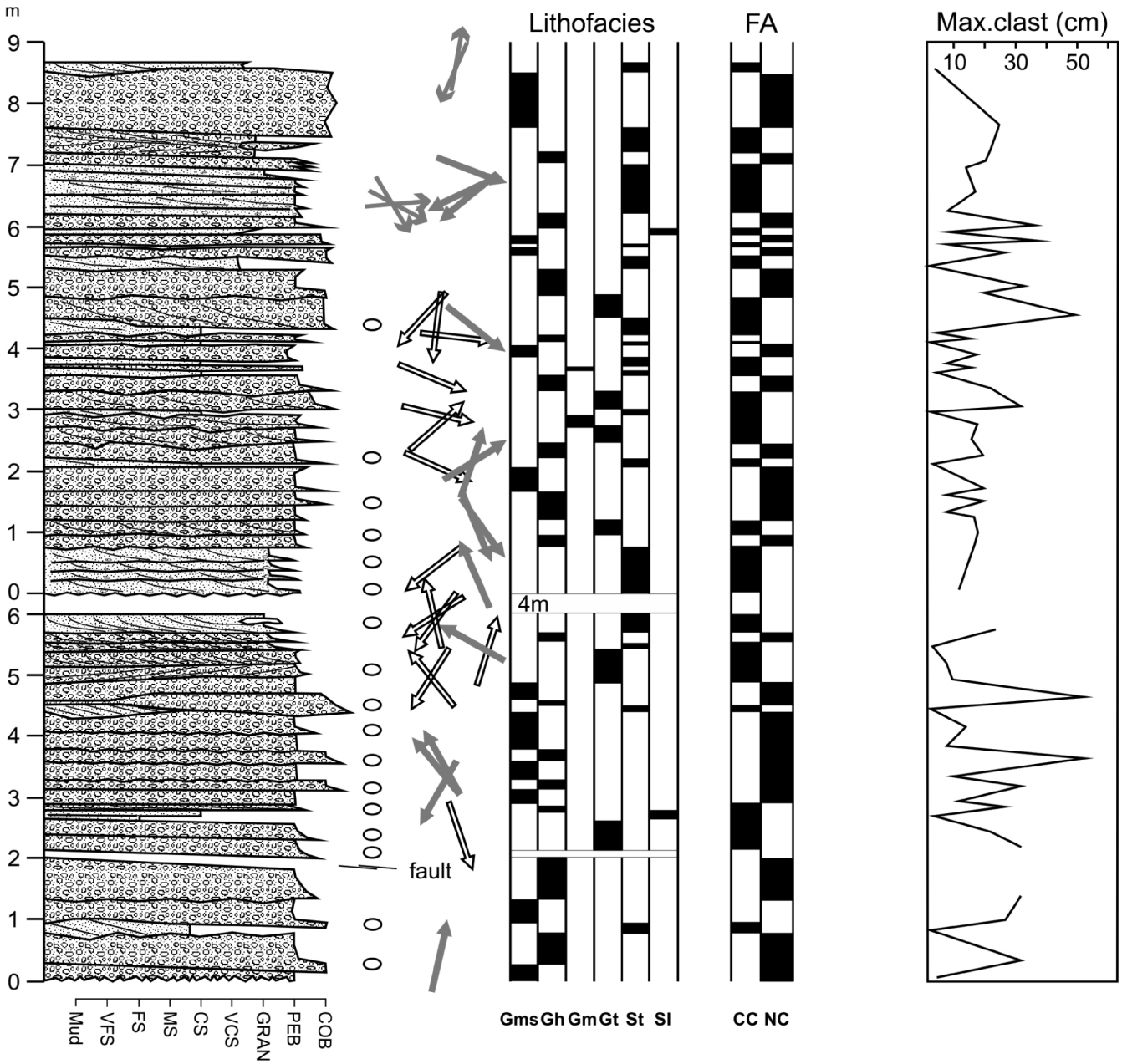

Figure 9H: Outcrop 7 (Heiligenstein Arkose Mb. - Heiligenstein Conglomerate Layers).

is very common. The beds have a tabular or wedge shape. The thickness of the association ranges from 30 cm to more than 4 m. The NC are predominantly formed by Gm, Gl, Gh or Gms facies. Nevertheless, significant variations in facies organisation have been recognised (the alternation of Gl and Gm or Gm and Gms facies, single facies (Gm, Gh, Gms) content. The NC were exceptionally formed by the alternation of sets of Sg and Gl facies. The thickness of individual sets also varies extraordinary (0.1 to 2.0 m). The uppermost part of the element is locally formed by thin (5-10 cm thick) planar beds of Sl, exceptionally Sp facies. The NC were recognized predominantly within the deposits of the Heiligenstein Arkose Mb., however their occurrence varies strongly (1.2% to 30.8% of the succession).

The NC were also rarely described within the Kalterbachgraben Sandstone/Siltstone Mb., where it represents 5.7% of the succession. A thin tabular bed of facies Gm with an erosive base and flat top formed here the basal part. This is followed by the dominant tabular beds of Sl facies with thin broadly lenticular interbeds of Sr facies.

Interpretation: The NC reflect deposition from subaerial sediment gravity flows/mass flows (cohesionless debris flows) and sheet flows. They are interpreted as the product of alluvial fan and alluvial plain systems. A single debris flow deposit can develop strong heterogeneity leading to a range of depositional textures and evolution (Nemec and Steel, 1984; Blair and McPherson, 1994). Variations in thickness and internal facies organisation are probably connected with the proximal-distal part of the alluvial fan. The cobbly and bouldery conglomerates of especially facies Gms (cohesionless debris flow) are interpreted as proximal parts, whereas facies Gh, Gl and Gm (hyperconcentrated flow, sheet flood, ephemeral stream flood) become increasingly important in the medial part of the fan. These conglomerates represent deposition on the active depositional lobes. The more distal examples comprise alternating conglomeratic and sandy facies (Sg and Gl). In general, there was a decrease in bed thickness and grain size, as well as a reduction of content, or even an absence of outsized clasts in the conglomerates in these „distal parts".

The local and thin non-channelized beds of predominantly Sl facies in the uppermost parts of the succession (superposition of cobbly or bouldery gravels), and the CC recognised in association with the NC, are connected with subsequent stream flows (channelized or non-channelized), which reworked the deposits of the alluvial fan. Such streams also reworked the abandoned fan sectors and their terminal parts. However, outwashing by running water and the washout tops of many layers indicate surface discharge or superficial flows as a significant process of fan evolution and the presence of more or less frequent precipitation (George and Berry, 1997; Harvey, 2004; Harvey et al., 2005; Roscher and Schneider, 2006; Kallmeier et al., 2010). The truncation of mass flow deposits was also common. These considerations suggest that precipitation events were relatively frequent and probably related to climate seasonality. Episodic sedimentation is a common feature of semi-arid to arid climates where sporadic rainfall combined with sparse vegetation leads to rapid pulses of run-off and sedimentation (Schumm, 1977; Bull, 1997). Thus the investigated fan and plain systems may be characterised as wet-type systems (George and Berry, 1997).

The absence of cohesive debris flows (mudflows), along with the absence of muddy intraclasts in the conglomerates (both

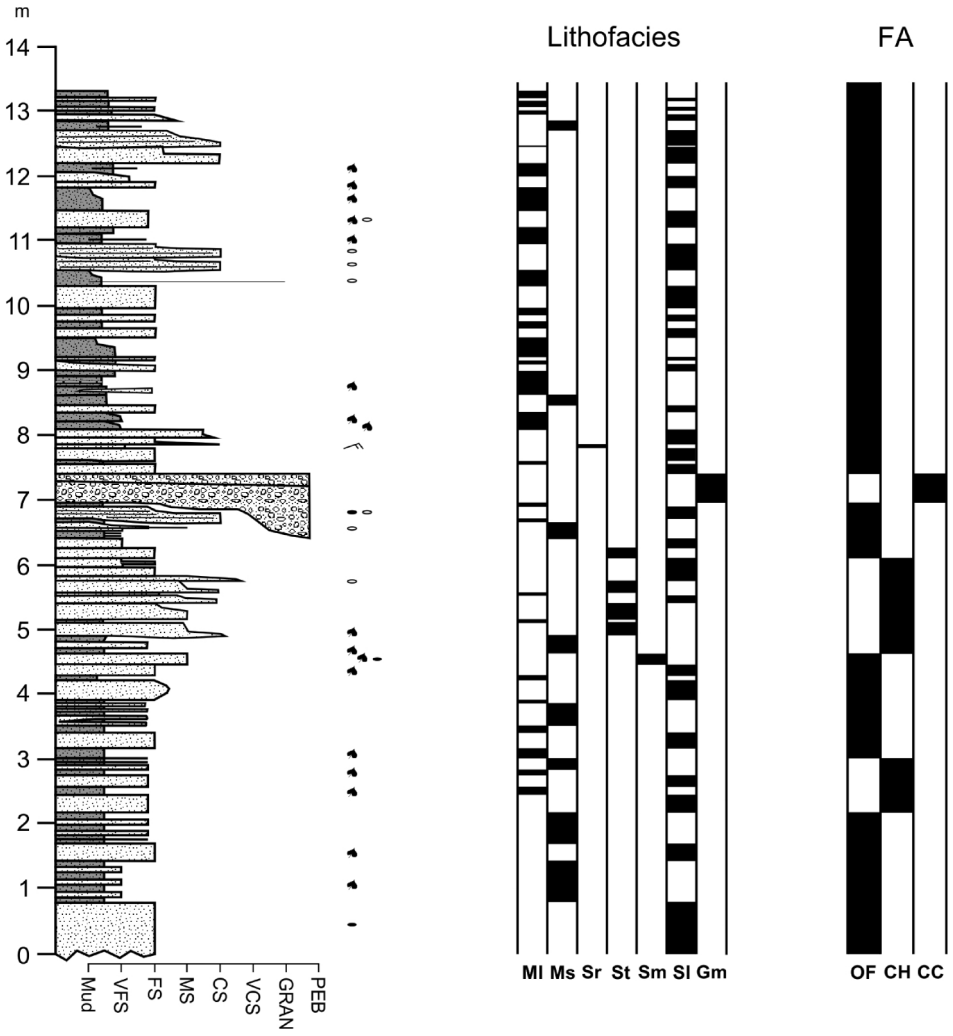

Figure 9l: Outcrop R (Kalterbachgraben Sandstone/Siltstone Mb.).

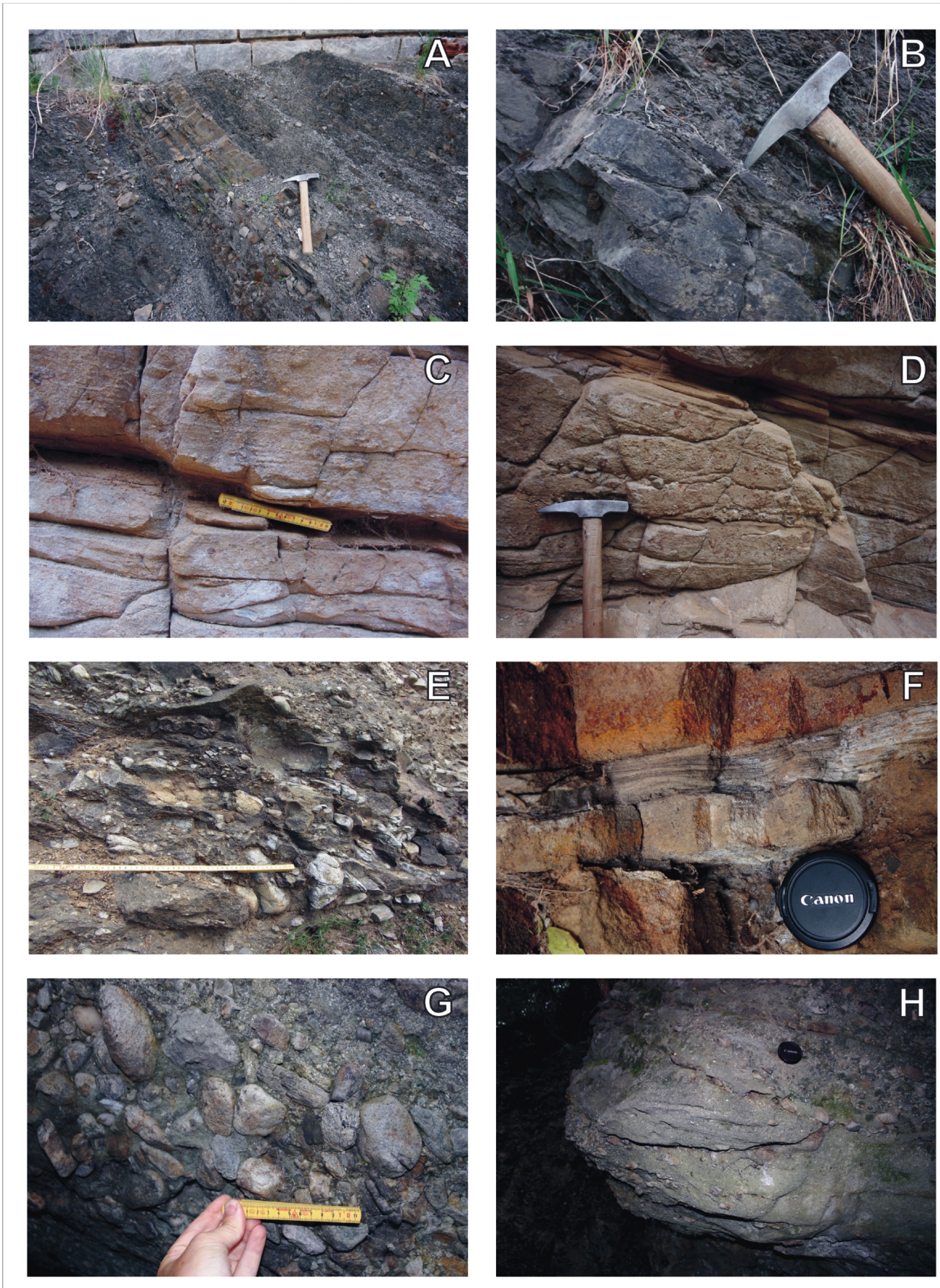

Figure 10: Structural and textural features of the studied deposits of the ZF. A: dominant non-channelized fine-grained deposits with interbed of channelized sandstones, B: deposits of channelized sandstones (facies St), C: deposits of facies Gl, D: deposits of facies Gms, E: deposits of facies Gm, F: deposits of facies Sl, G: clast supported conglomerates, H: alternation of beds of facies St and Gt.

CC and NC) of the Heiligenstein Arkose Mb. and the dominance of water-laden flows, all point to climatic condition and rock composition in the source area. The clay-deficiency can be connected with rapid erosion and redeposition of the weathered material under an arid or semi-arid climate (Blair and McPherson, 1994).

4.7 Paleocurrent Analysis

The paleocurrent results (Fig. 12) reveal a complex pattern of the paleotransport within the studied area, as well as in the individual outcrops. The differences in orientation of pebble imbrication, foresets of cross-stratification, accretional surfaces and channel axis are typical for highly mobile, rapidly shifting bedforms, channels with highly varying water discharge and depositional environments with very low morphology (Ramos and Sopeña, 1983).

The orientation of the channel axes is generally towards N and NE, rarely towards WNW or ESE. The accretion surfaces are often oriented towards NE or SW, that is parallel or perpendicular to the channel axes. The explanation for such a relationship could be connected with the curved channel morphology or the differences in fluvial discharge (Bridge, 1993).

The orientation of the foresets of cross-stratification is very complex with significant scattering even at a single outcrop. The orientation of the foresets is generally parallel, oblique and also perpendicular to the channel axes or accretion surfaces.

Two types of preferred orientation of elongated pebbles could be recognised in outcrops (i.e. perpendicular or parallel to the stratification or channel axis). If we apply such a position, the direction of orientation is commonly NE and SE, less commonly towards NNW.

Interpretation: The combination of paleocurrent indicators reflects that the general transport direction within the studied area was from SE towards NW, N and NE.

The combination of parallel, oblique and perpendicular orientation of stratification towards both channel axes and accretion surfaces is interpreted as the result of both downstream- and lateral-accretion (Miall, 1996). The evidence of the lateral accretion indicates the lateral growth and modification of channel bars (Ramos and Sopeña, 1983; Kostic and Aigner, 2007). We presume that the highly complex orientation of the paleocurrent was strongly influenced by a relatively flat relief of the depositional area.

5. Depositional model and discussion

The limited lateral and vertical extents of the outcrops preclude the precise recognition of the lateral distribution of facies associations and make difficult to define spatial and up-

Figure 11: Structural and textural features of the studied deposits of the ZF. A: channel (channelized conglomerates) cut into non-channelized fine-grained deposits, B: outsized boulders within conglomerates of facies Gms, C: alternation of beds of facies Gms and Sl, D: deposits of facies Ml.

ward trends of the succession.

Generally, the finning upward trend was recognised in several successions, where either deposits of channelized conglomerates or sandstones were followed by deposits of floodplain, or non-channelized conglomerates were followed by channelized deposits, sometimes even with floodplain deposits on the top. Moreover the floodplain deposits were multiply eroded by the debris flows. However, we do not recognise the "typical" meandering fluvial system in association with floodplain deposits and also the braided fluvial pattern in the channels was not very common. Thus on the outcrop scale we can propose the deposition which reveal a vertical and possibly lateral transition from the proximal deposits with non-channelized conglomerates to the distal part with channelized deposits and, finally, to the very distal fine-grained deposits (Fig. 13).

Moreover, some variations in the depositional style and environment within the individual members of the Zöbing Formation can be recognised, which are partly similar to the previously mentioned proximal to distal variations on a much smaller outcrops scale. Although sediment supply and discharge would be expected to be punctuated, the heterogeneity of deposits with respect to the thickness, stacking patterns and facies distribution throughout the succession suggests that the magnitude, discharge and sediment supply fluctuate significantly over time. The spatial and temporal evolution of the ZF is characterised by: (i) initial deposition in the basin – the evolution of the floodplain with a distal fluvial influence (the Leopoldacker Siltstone Mb., the Rockenbauer Sandstone Mb.); (ii) the progradation of the fluvial system into the floodplain, avulsion of the channels (the Kalterbachgraben Sandstone/Siltstone Mb., the Kampbrücke Siltstone Mb.); (iii) the advance phase with progradation of alluvial fan and proximal fluvial channels (the Heiligenstein Arkose Mb.); and (iv) the final retrogradation of the alluvial/fluvial system back towards the hinterland (the Lamm Siltstone/Arkose Mb., the Geißberg Sandstone Mb.).

Recognised progradational/retrogradational cycles of varied scale probably reflect a combined effect of autocyclic (possibly outcrop scale) and allocyclic factors (possibly the scale of the complete formation). The intrinsic (autocyclic) processes can be connected with channel avulsion and the alternation of channelized deposits with floodplain mudstones. The extrinsic (allocyclic) processes are connected with tectonic processes forming the accommodation space. Based on these assumptions, we must discuss the evolution of the three recognised depositional environments, which were laterally connected, i.e. alluvial fan, coarse grained fluvial channels and floodplain deposits/overbank fines.

There are significant differences in the definition of alluvial fan, especially concerning participation of water flow processes in this depositional environment (Stanistreet and McCarthy, 1993; Blair and McPherson, 1994; Miall, 1996). The characteristics of alluvial fans are determined by a number of inter-

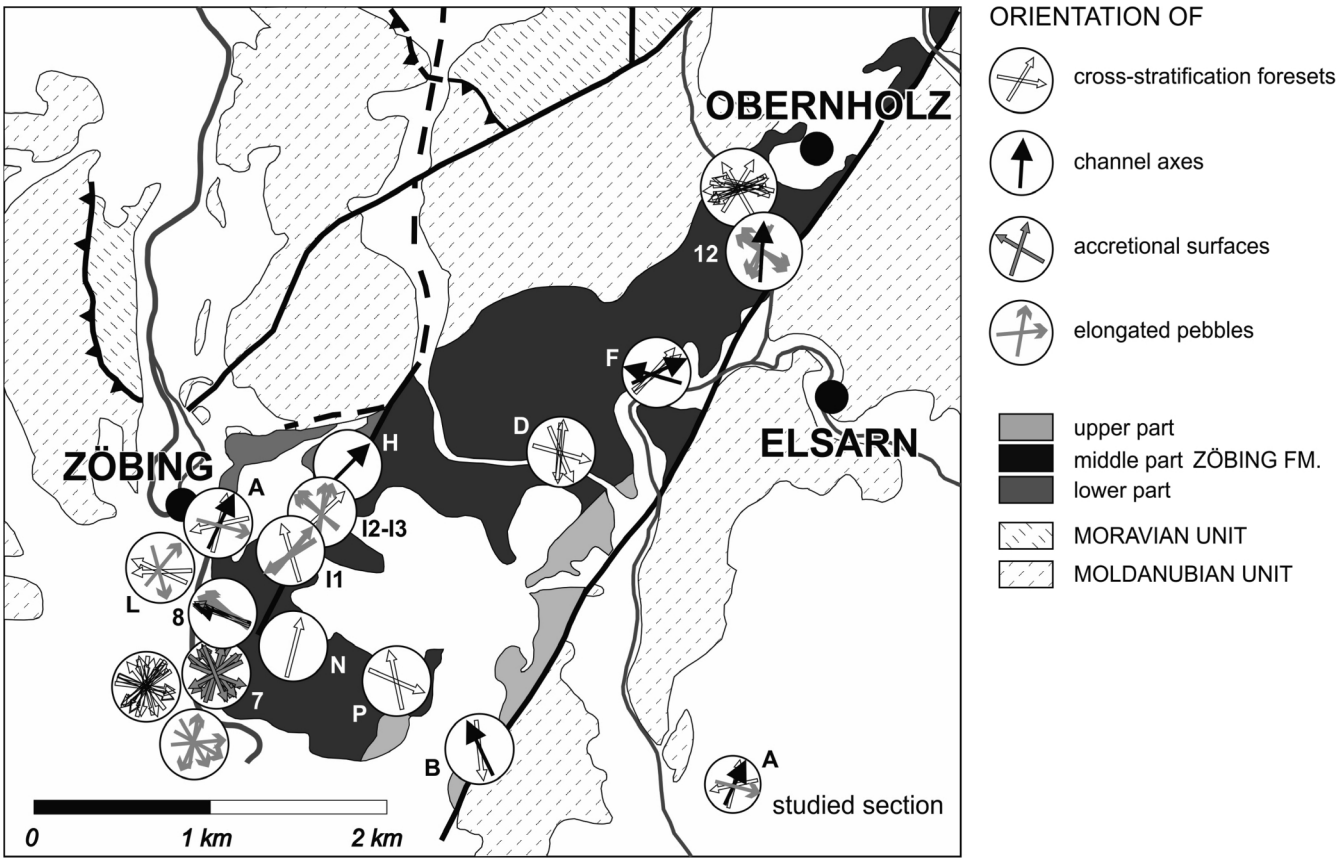

Figure 12: Paleocurrent orientations for the deposits of the Zöbing Formation.

related factors, although tectonic activity and climatic changes are thought to be the main factors responsible for the occurrence of cyclic patterns in sedimentation, which are alternate phases of progradation, aggradation and retrogradation (Fraser and DeCelles, 1992; Dorn, 1994; Viseras et al., 2003; Harvey, 2004; Amorosi et al., 2008; Cain and Mountney, 2009).

Tectonic processes may cause uplift, tilting, channel incision and the narrowing of the catchment outlets (Leeder, 1999), thus providing the accommodation space that is necessary for sediment accumulation and often promoting fan aggradation (DeCelles et al., 1991; Viseras et al., 2003). The initiation of the deposition of coarse-grained clastics of the Heiligenstein Arkose Mb. may be interpreted as a signal for the (re)activation of faults.

The significant variations in thickness and width of the observed channels and complex infill suggest substantial changes in water discharge. Such observations are commonly connected with the role of climate, which affected the rate of sediment transport, relief equilibrium and fan geometry (Dorn, 1994; Ritter et al., 1995). However, a clear distinction between climatic and tectonic signals is difficult. In addition to tectonic and climatic determinations, fan evolution is influenced by processes such as catchment area evolution and autocyclic lobe switching (Fraser and DeCelles, 1992; Blair and McPherson, 1994; Huerta et al., 2011).

The recognised instability in the channel position and the significant variations in the fluvial discharge both point to an avulsive pattern of water flow. Avulsion is responsible for the relatively rapid transfer of river flow out of an established section of channel into a new flow pathway on the flood plain. Stacked channel fills indicate the repeated reoccupation of the same site by avulsing channels and inherited flood plain topography. Large fluctuations in discharge may be responsible for the rapid avulsive pattern of channel relocation. Episodic flood events accompanied by an increase in overall discharge may indicate the rapid aggradation of channels and subsequent avulsion (Wells and Dorr, 1987; Jones and Schumm, 1999). The depositional events on Quaternary alluvial fans in arid/semi-arid areas show their effects on the scale of year and decades (Harvey et al., 2005). Higher rates of deposition would possibly suggest a pronounced seasonality in the predominantly dry Permian climate (Roscher and Schneider, 2006).

Overbank deposits are often interpreted as evidence of fluvial, especially meandering style (Miall, 1985). However, Desloges and Church (1987), Mack and Seager (1990) or Bentham et al. (1993) reported ancient coarse-grained braided systems containing significant amounts of preserved floodplain material. Similar deposits were interpreted by Hampton and Horton (2007) as a product of a sheetflow-dominated system connected with fluvial fan conditions in an arid to semi-arid climate with possibly seasonal and strongly fluctuating water discharge (Hogg, 1982). The proposed explanation for the enhanced floodplain preservation in the studied sediment accumulation associated with coarse-grained braided fluvial deposits or fluvial fan could be rapid regional subsidence over extended periods of time (Bentham et al., 1993; Bridge and Leeder, 1979; Kraus and Middleton, 1987; Shuster and Steidtmann, 1987). Such conditions and a relatively arid, seasonal climate are critical for promoting the generation of sheet flow-dominated fluvial systems with brief pulses of rapid sedimentation, primarily on unconfined (non-channelized) plains, as well as locally in broad, poorly confined channels (Bromley, 1991), where sediment tends to aggrade rather than be distributed by lateral or downslope migration (Hampton and Horton, 2007).

The depositional model for the Zöbing Formation should include all the recognised depositional environments, allow both rapid and systematic transition in behaviour and depositional morphology from proximal regions to distal ones, and include the existence and evolution of fluvial channels and extended floodplain. The proposed depositional system (Fig. 13) combines models of alluvial fan with models of a terminal fan/fluvial distributary system (Nichols and Fischer, 2007). The terminal fluvial systems, which develop under the influence of semi-arid to arid climatic regimes represent a style in which the termination of channelized fluvial flow occurs before a significant standing body of water is reached. Distributive fluvial systems are fan-like systems in which multiple channels co-exist and distribute water and sediment across the fan (Weissmann et al., 2010). For that reason mostly small channel bodies with a limited range of dimensions are preserved at the expense of outsized channels (Weissmann et al., 2010; Fielding et al., 2012). It is possible, that terminal fans were relics of a more arid climate and that a tributary fluvial system was developed during a more humid period. The absence of a large fluvial system can be explained by the restricted depositional space of the graben or half-graben type of the basin.

6. Conclusions

The erosional remnants of the continental Permo-Carbonife-

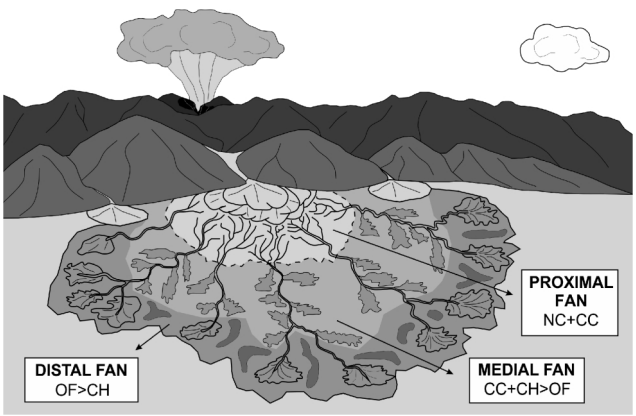

Figure 13: Hypothetical reconstruction of the depositional system of the Zöbing Formation with volcanic activity in the hinterland. Explanation to the symbols: NC: non-channelized conglomerates, CC: channelized conglomerates, CH: channelized sandstones, OF: non-channelized fine-grained deposits.

rous deposits of the Zöbing Formation in Lower Austria were studied in 34 relatively small outcrops. Fourteen lithofacies have been identified and further grouped into four associations i.e. (a) non-channelized fine-grained deposits; (b) channelized sandstones, (c) non-channelized conglomerates, and (d) channelized conglomerates. Occurrences of these facies associations vary within individual members of the Zöbing Formation. Non-channelized fine-grained deposits are interpreted as a product of deposition on floodplains. Channelized sandstones are connected with fluvial processes and mostly represent crevasse channels cut into the floodplains. Channelized conglomerates originated from coarse-grained confined/channelized water/stream flows and hyperconcentrated flows. Non-channelized conglomerates are interpreted as product of cohesionless debris flows and sheet flows within alluvial fan and alluvial plain systems. A close association of non-channelized and channelized conglomerates and floodplain deposits points to a coarse-grained fluvial system or fluvial fan accompanied by an extended floodplain. A terminal fluvial systems developed under the influence of semiarid to arid climatic regimes is supposed to be the depositional environment of the Zöbing Formation.

Absence of both the deposits of cohesive debris flows and muddy intraclasts in conglomerates, together with the dominance of deposits of water-flows over deposits of debris flows, all point to rapid physical erosion and redeposition in the source area, where acidic magmatic and metamorphic rocks dominated. The petrographical and geochemical study confirms that the detritus of the Upper Palaeozoic deposits was mostly derived from primary sources formed by crystalline rocks (particularly metapelitic rocks - mica schists, paragneisses, felsitic granulites, and also magmatic rocks). The source area was predominantly located in the Moldanubian unit.

The general provenance evolution over time does not indicate the successive exhumation of a simple structured orogen but may be interpreted as differences in expansion in the source areas. The basal successions are characterised by material from local/adjacent sources whereas for the younger parts of the successions a wider provenance and variations in primary and recycled detritus are assumed. The source areas seem to be largely stable during the depositional history, reflecting the tectonic history and depositional phases.

Acknowledgement

The authors wish to thank the Grants Agency of the Czech Republic No. 205/09/1257 and 205/09/0103, which kindly sponsored the costs of the analytical data. The field work was generously sponsored by the Geological Survey of Austria. We are grateful to Fritz F. Steininger for his help during field work and stratigraphic issues, to Maria Heinrich for providing field data and to R. Melichar for restoration of the directional data. We also give thanks for helpful comments to two anonymous reviewers.

References

Adhikari, B.R. and Wagreich, M., 2011. Provenance evolution of collapse graben fill in the Himalaya - The Miocene to Quaternary Thakkhola-Mustang graben (Nepal). Sedimentary Geology, 233, 1-14. http://dx.doi.org/10.1016/j.sedgeo.2010.09.021

Amorosi, A., Pavesi, M., Ricci Lucci, M., Sarti, G. and Piccin, A., 2008. Climatic signature of cyclic fluvial architecture from the Quaternary of the central Po Plain, Italy. Sedimentary Geology, 209, 58-68. http://dx.doi.org/10.1016/j.sedgeo.2008.06.010

Baas, J.H., 2000. EZ-ROSE: a computer program for equal-area circular histograms and statistical analysis of two-dimensional vectorial data. Computers and Geosciences, 26, 153-166.

Bachmayer, F. and Vasicek, W., 1967. Insektenreste aus dem Perm von Zöbing bei Krems in Niederrösterreich. Annalen des Naturhistorischen Museums Wien, 71, 13-18.

Bahlburg, H., 1998. The geochemistry and provenance of Ordovician turbidites in the Argentine Puna. In: R.J. Pankhurst and C.W. Rapela (eds.), The Proto-Andean Margin of Gondwana. Geological Society of London, Special Publication, 142, pp. 127-142.

Bentham, P.A., Talling, P.J. and Burbank, D.W., 1993. Braided stream and flood-plain deposition in a rapidly aggrading basin: the Escanilla formation, Spanish Pyrenees. In: J.L. Best and C.S. Bristow (eds.), Braided Rivers. Geological Society of London, Special Publication, 75, pp. 177-194.

Berger, W., 1951. Neue Pflanzenfunde aus dem Rotliegenden von Zöbing (Niederösterreich). Anzeiger der österreichischen Akademie der Wissenschaften, mathematisch-naturwissenschaftliche Klasse, 88/11, 288-295.

Bhatia, M.R. and Crook, K.A.W., 1986. Trace element characteristics of graywackes and tectonic setting discrimination of sedimentary basins. Contributions to Mineralogy and Petrology, 92, 181-193.

Blair, T.C. and McPherson, J.C., 1994. Alluvial fans and their natural distinction from rivers based on morphology, hydraulic processes, sedimentary processes, and facies assemblages. Journal of Sedimentary Research, A64, 450-489.

Bock, B., McLennan, S.M. and Hanson, G.N., 1998. Geochemistry and provenance of the Middle Ordovician Austin Glen Member (Normanskill Formation) and the Taconian Orogeny in New England. Sedimentology, 45, 635-655.

Borges, J. and Huh, Y., 2007. Petrography and chemistry of the bed sediments of the Red River in China and Vietnam: provenance and chemical weathering. Sedimentary Geology, 194, 155-168. http://dx.doi.org/10.1016/j.sedgeo.2006.05.029

Brayshaw, A.C., 1984. Characteristics and Origin of Cluster Bedforms in Coarse-Grained Alluvial Channels. In: E.H. Kostner and R.J. Steel (eds.), Sedimentology of Gravels and Conglomerates. Canadian Society of Petroleum Geologists, Memoir 10, pp. 77-85.

Bridge, J.S., 1993. Description and Interpretation of fluvial deposits: a critical perspective. Sedimentology, 40, 801-810.

Bridge, J.S. and Leeder, M.R., 1979. A simulation model of allu-

vial stratigraphy. Sedimentology, 26, 617-644.

Bromley, M.H., 1991. Variations in fluvial style as revealed by architectural elements, Kayenta Formation, Mesa Creek, Colorado, USA: Evidence for both ephemeral and perennial fluvial processes. In: A. D. Miall, and N. Tyler (eds.), The three-dimensional facies architecture of terrigeneous clastic sediments and its implications for hydrocarbon discovery and recovery. SEPM, Concepts in Sedimentology and Paleontology, 3, pp. 94-102.

Bull, W.B., 1997. Discontinuous ephemeral streams. Geomorphology, 19, 227-276.

Cain, S.A. and Mountney, N.P., 2009. Spatial and temporal evolution of a terminal fluvial fan system: the Permian Organ Rock Formation, South-east Utah, USA. Sedimentology, 56, 1774-1800. http://dx.doi.org/10.1111/j.1365-3091.2009.01057.x

Cascalho, J. and Fradique, C., 2007. The sources and hydraulic sorting of heavy minerals on the northern Portuguese continental margin. Developments in Sedimentology, 58, 75-107. http://dx.doi.org/10.1016/S0070-4571(07)58003-9

Cheel, R.J. and Middleton, G.V., 1986. Horizontal lamination formed under upper flow regime plane bed conditions. Journal of Geology, 94, 489-504.

Cichocki, O., Popovtschak, M., Szameit, E. and Vasicek, W., 1991. Excursion A, 22. September 1991: Northern Lower Austria. In: J. Kovar-Eder (ed.), Palaeovegetational development of Europe. Pan-European Palaeobotanical Conference, Wien. Field-Guide, pp. 5-22.

Collinson, J.D. and Thompson, D.B., 1982. Sedimentary structures. Allen and Unwin, 194 pp.

Corcoran, P.L., 2005. Recycling and chemical weathering in tectonically controlled Mesozoic-Cenozoic basins of New Zealand. Sedimentology, 52, 757-774. http://dx.doi.org/10.1111/j.1365-3091.2005.00723.x

Cox, R. and Lowe, D.R., 1995. A conceptual review of regional-scale controls on the composition of clastic sediment and the co-evolution of continental blocks and their sedimentary cover. Journal of Sedimentary Research, A65/1, 548-558.

Čžjžek, J., 1849. Geognostische Karte der Umgebungen von Krems und vom Manhardsberge. Maßstab 1:72.000, Wien.

Čžjžek, J., 1853. Erläuterungen zur geologischen Karte der Umgebungen von Krems und vom Manhartsberg. Sitzungsberichte der k.k. Akademie der Wissenschaften, mathematisch-naturwissenschaftliche Classe, Beilage 7, 77 pp.

DeCelles, P.G., Gray, M.B., Ridgway, K.D., Cole, R.B., Pivnik, D.A., Pequera, N. and Srivastava, P., 1991. Controls on synorogenic alluvial-fan architecture, Beartooth Conglomerate (Palaeocene), Wyoming and Montana. Sedimentology, 38, 567-590.

Desloges, J.R. and Church, M., 1987. Channel and floodplain facies in a wandering gravel-bed river. In: F.G. Etheridge, R.M. Flores and M.D. Harvey (eds.), Recent Developments in Fluvial Sedimentology. SEPM Special Publications, 39, pp. 99-110.

Dickinson, W. R., 1990. Clastic Petrofacies. In: A. D. Miall (ed.), Principles of Sedimentary Basin Analysis. Springer New York, pp. 1-668.

Dickinson, W. R. and Suczek, Ch. A., 1979. Plate tectonics and sandstone composition. The American Association of Petroleum Geologists, Bulletin, 63/12, 2164-2182.

Dickinson, W. R. and Valloni, R., 1980. Plate settings and provenance of sands in modern ocean basins. Geology, 8/2, 82-86.

Dorn, R.I., 1994. The role of climatic change in alluvial fan development. In: A.D. Abrahams and A.J. Parsons (eds.), Geomorphology of desert environments. Chapman and Hall, London, pp. 593-615.

Einsele, G., 1992. Sedimentary Basins: Evolution, Facies, and Sediment Budget. Springer Berlin, 628 pp.

Ettingshausen, C.v., 1852. Beitrag zur näheren Kenntniss der Flora der Wealdenperiode. Abhandlungen der k.k. Geologischen Reichsanstalt, 1/3, 1-32.

Eynatten, H. von and Gaupp, R., 1999. Provenance of Cretaceous synorogenic sandstones in the Eastern Alps: constraints from framework petrography, heavy mineral analysis and mineral chemistry. Sedimentary Geology, 124, 81-111.

Fedo, C. M., Nesbitt, H.W. and Young, G.M., 1995. Unraveling the effects of potassium metasomatism in sedimentary rocks and paleosols, with implications for paleoweathering conditions and provenance. Geology, 23, 921-924.

Fielding, C.R., Ashworth, P.J., Best, J.L., Prokocki, E.W. and Sambrook Smith, G.H., 2012. Tributary, distributary and other fluvial patterns: What really represents the norm in the continental rock record? Sedimentary Geology, 261–262, 15-32. http://dx.doi.org/10.1016/j.sedgeo.2012.03.004

Finger, F. and Haunschmid, B., 1988. Die mikroskopische Untersuchung der akzessorischen Zirkone als Methode zur Klärung der Intrusionsfolge in Granitgebieten - eine Studie im nordöstlichen oberösterreichischen Moldanubikum. Jahrbuch der Geologischen Bundesanstalt, 131/2, 255-266.

Fisher, J.A., Nichols, G.J. and Waltham, D.A., 2007. Unconfined flow deposits in distal sectors of fluvial distributary systems: Examples from the Miocene Luna and Huesca Systems, northern Spain. Sedimentary Geology, 195/1-2, 55-73. http://dx.doi.org/10.1016/j.sedgeo.2006.07.005

Flügel, E., 1960. Nichtmarine Muscheln aus dem Jungpaläozoikum von Zöbing (Niederösterreich). Verhandlungen der Geologischen Bundesanstalt, 1960/1, 78-82.

Force, E.R., 1980. The provenance of rutile. Journal of Sedimentary Research, 50/2, 485-488.

Fraser, G.S. and DeCelles, P.G., 1992. Geomorphic controls on sediment accumulation at margins of foreland basins. Basin Research, 4, 233-252.

Frasl, G., Fuchs, G., Höck, V., Roetzel, R., Steininger, F., Vasicek, W. and Vetters, W., 1991. Geologische Karte Blatt 21 Horn. Unpublished map 1:25.000, Archiv Geologische Bundesanstalt, Archiv-Nr. A08063-ÖK25V/21-3, Wien.

Fuchs, W., Grill, R., Matura, A. and Vasicek, W., 1984. Geologische Karte der Republik Österreich 1:50.000. 38 Krems. Geologische Bundesanstalt.

Garver, J. I., Royce, P. R. and Smick, T. A., 1996. Chromium and Nickel in Shale of the Taconic Foreland: A Case Study for the Provenance of Fine-Grained Sediments with an Ultramafic Source. Journal of Sedimentary Research, 66, 100-106.

Garzanti, E. and Andò, S., 2007. Heavy mineral concentration in modern sands: implications for provenance interpretation. In: M.A. Mange and D.T. Wright (eds.), Heavy Minerals in Use. Developments in Sedimentology, 58, pp. 517-545.

George, G.T. and Berry, J.K., 1997. Permian (Upper Rotliegend) synsedimentary tectonics, basin development and palaeogeography of the southern North Sea. In: K. Ziegler, P. Turner and S.R. Daines (eds.), Petroleum Geology of the Southern North Sea: Future Potential. Geological Society Special Publication, 123, pp. 31-61.

Gu, X.X., Liu, J.M., Zheng, M.H., Tang, J.X. and Qi, L., 2002. Provenance and tectonic setting of the Proterozoic turbidites in Hunan, South China: geochemical evidence. Journal of Sedimentary Research, 72, 393-407. http://dx.doi.org/10.1306/081601720393

Hallsworth, C.R. and Chisholm, J.I., 2008. Provenance of late Carboniferous sandstones in the Pennine Basin (UK) from combined heavy mineral, garnet geochemistry and paleocurrent studies. Sedimentary Geology, 203, 196-212. http://dx.doi.org/10.1016/j.sedgeo.2007.11.002

Hampton, B.A. and Horton, B.K., 2007. Sheetflow fluvial processes in a rapidly subsiding basin, Altiplano plateau, Bolivia. Sedimentology, 54, 1121-1148. http://dx.doi.org/10.1111/j.1365-3091.2007.00875.x

Harms, J.C., Southard, J.B., Spearing, D.R. and Walker, R.G., 1975. Depositional Environments as Interpreted from Primary Sedimentary Structures and Stratification Sequences. SEPM Short Course No. 2, Lecture Notes, Society of Economic Paleontologists and Mineralogists, 1-161, Dallas.

Harvey, A.M., 2004. The response of dry-region alluvial fans to late Quaternary climatic change. In: A.S. Alsharhan, W.W. Wood, A.S. Goudie, A. Fowler and E.M. Abdellatif (eds.), Desertification in the Third Millenium. Balkema Rotterdam, pp. 83-98.

Harvey, A.M., Mather, A.E. and Stokes, M., 2005. Alluvial fans: geomorphology, sedimentology, dynamics — introduction. A review of alluvial-fan research. In: A.M. Harvey, A.E. Mather and M. Stokes (eds.), Alluvial Fans: Geomorphology, Sedimentology, Dynamics. Geological Society, London, Special Publications, 251, pp. 1-7.

Heinrich M. (ed.), Atzenhofer, B., Havlíček, P., Holásek, O., Klein, P., Lipiarska, I., Lipiarski, P., Rabeder, J., Roetzel, R., Untersweg, Th., Vachek, M. and Wimmer-Frey, I., 2008. Geologische Detailkarte des Weinbaugebietes Kamptal 1:10.000. 25 maps, CD with documentation and outline map, Geologische Bundesanstalt on behalf of Weinkomitee Kamptal, Wien.

Herron, M.M., 1988. Geochemical classification of terrigenous sands and shales from core and log data. Journal of Sedimentary Petrology, 58, 820-829.

Hjellbakk, A., 1997. Facies and fluvial architecture of a high-energy braided river: the Upper Proterozoic Seglodden Member, Varanger Peninsula, northern Norway. Sedimentary Geology, 114, 131–161.

Hogg, S.E., 1982. Sheetfloods, sheetwash, sheetflow, or ... ? Earth-Science Review, 18, 59-76.

Holger, Ph. A. Ritter v., 1842. Geognostische Karte des Kreises ob dem Manhartsberge in Oesterreich unter der Ens, nebst einer kurzen Beschreibung der daselbst vorkommenden Felsarten. 44 p., 1 geol. map (1841).

Hoppe, G., 1966. Zirkone aus Granuliten. Berichte der Deutschen Gesellschaft für Geologische Wissenschaften - Reihe B: Mineralogie und Lagerstättenforschung, 11/1, 47-81.

Hubert, J.F., 1962. A zircon-tourmaline-rutile maturity index and the interdependence of the composition of heavy mineral assemblages with the gross composition and texture of sandstones. Journal of Sedimentary Petrology, 32/3, 440-450.

Huerta, P., Armenteros, I. and Silva, P.G., 2011. Large-scale architecture in non-marine basins: the response to the interplay between accommodation space and sediment supply. Sedimentology, 58, 1716-1736. http://dx.doi.org/10.1111/j.1365-3091.2011.01231.x

Ingersoll, R. V., 1990. Actualistic sandstone petrofacies: Discriminating modern and ancient source rocks. Geology, 18, 733-736.

Jo, H.R. and Chough, S.K., 2001. Architectural analysis of fluvial sequences in the southwestern part of Kyonsang Basin (Early Cretaceous), SE Korea. Sedimentary Geology, 144/3-4, 307-334. http://dx.doi.org/10.1016/S0037-0738(01)00123-3

Jones, L.S. and Schumm, S.A., 1999. Causes of avulsion: an overview. In: N.D. Smith and J. Rogers (eds.), Fluvial Sedimentology VI. International Association of Sedimentologists, Special Publication, 28, pp. 171-178.

Kallmeier, E., Breitkreuz, C., Kiersnowski, H. and Geißler, M., 2010. Issues associated with the distinction between climatic and tectonic controls on Permian alluvial fan deposits from the Kotzen and Barnim Basins (North German Basin). Sedimentary Geology, 223, 15-34. http://dx.doi.org/10.1016/j.sedgeo.2009.09.009

Kalvoda, J., Bábek, O., Fatka, O., Leichmann, J., Melichar, R., Nehyba, S. and Špaček, P., 2008. Brunovistulian terrane (Bohemian Massif, Central Europe) from late Proterozoic to late Paleozoic: a review. International Journal of Earth Sciences, 97, 497-517. http://dx.doi.org/10.1007/s00531-007-0183-1

Kamenetsky, V.S., Crawford, A.J. and Meffre, S., 2001. Factors controlling chemistry of magmatic spinel: an empirical study of associated olivine, Cr-spinel and melt inclusions from primitive rocks. Journal of Petrology, 42, 655-671. http://dx.doi.org/10.1093/petrology/42.4.655

Kostic, B. and Aigner, T., 2007. Sedimentary architecture and 3D ground-penetrating radar analysis of gravelly meandering river deposits (Neckar Valley, SW Germany). Sedimentology, 54, 789-808. http://dx.doi.org/10.1111/j.1365-3091.2007.00860.x

Krainer, K., 1993. Late- and Post-Variscan Sediments of the Eastern and Southern Alps. In: J.F. von Raumer, and F. Neubauer (eds.), Pre-Mesozoic Geology in the Alps. pp. 537-564.

Kraus, M. and Middleton, L.T., 1987. Contrasting architecture of two alluvial suites in different structural settings. In: F.G. Ethridge, R.M. Flores and M.D. Harvey (eds.), Recent developments in Fluvial Sedimentology. Society of Economic Paleontologists and Mineralogists, Special Publication, 39, pp. 253-262.

Larsen, V. and Steel, R.J., 1978. The sedimentary history of a debris flow-dominated alluvial fan - a study of textural inversion. Sedimentology, 25, 37-59.

Leeder, M.R., 1999. Sedimentology and Sedimentary Basins: From Turbulence to Tectonics. Blackwell Science Ltd., Oxford, 608 pp.

Lihou, J.C. and Mange-Rajetzky, M.A., 1996. Provenance of the Sardona Flysch, eastern Swiss Alps: example of high-resolution heavy mineral analysis applied to an ultrastable assemblage. Sedimentary Geology, 105, 141-157.

López-Gómez, J., Martín-Chivelet, J. and Palma, R. M., 2009. Architecture and development of the alluvial sediments of the Upper Jurassic Tordillo Formation in the Cañada Ancha Valley, northern Neuquén Basin, Argentina. Sedimentary Geology, 219, 180-195. http://dx.doi.org/10.1016/j.sedgeo.2009.05.006

Mack, G.H. and Seager, W.R., 1990. Tectonic control on facies distribution of the Camp Rice and Palomas Formations (Plio-Pleistocene) in the southern Rio Grande rift. Geological Society of America, Bulletin, 102, 45-53.

Mack, G.H., Leeder, M., Perez-Arlucea, M. and Bailey, B.D.J., 2003. Early Permian silt-bed fluvial sedimentation in the Orogrande basin of the Ancestral Rocky Mountains, New Mexico, USA. Sedimentary Geology, 160, 159-178. http://dx.doi.org/10.1016/S0037-0738(02)00375-5

Mader, D., 1980. Weitergewachsene Zirkone im Bundsandstein der Westeifel. Der Aufschluss, 31, 163-170.

Maizels, J., 1989. Sedimentology, paleoflow dynamics and flood history of jökulhlaup deposits: paleohydrology of Holocene sediment sequences in southern Iceland sandur deposits. Journal of Sedimentary Petrology, 59, 204-223.

Maizels, J.K., 1993. Lithofacies variations within sandur deposits: the role of runoff regime, flow dynamics and sediment supply characteristics. Sedimentary Geology, 85, 299-325.

McCann, T., Pascal, C., Timmerman, M.J., Krzywiec, P., López-Gómez, J., Wetzel, A., Krawczyk, C.M., H. Rieke, H. and Lamarche, J., 2006. Post-Variscan (end Carboniferous-Early Permian) basin evolution in Western and Central Europe. In: D.G. Gee and R.A. Stephenson (eds.), European Lithosphere Dynamics. Geological Society, London, Memoirs, 32, pp. 355–388.

McLennan, S.M., Hemming, S., McDaniel, D.K. and Hanson, G. N., 1993. Geochemical approaches to sedimentation, provenance, and tectonics. In: M.J. Johnsson and A. Basu (eds.), Processes controlling the composition of clastic sediments. Geological Society of America, Special Papers, 284, pp. 21-40.

Meinhold, G., Anders, B., Kostopoulos, D. and Reischmann, T., 2008. Rutile chemistry and thermometry as provenance indicator: An example from Chios Island, Greece. Sedimentary Geology, 203, 98-111. http://dx.doi.org/10.1016/j.sedgeo.2007.11.004

Miall, A.D., 1985. Architectural-element analysis: a new method of facies analysis applied to fluvial deposits. Earth-Science Review, 22, 261-308.

Miall, A.D., 1989. Architectural elements and bounding surfaces in channelized clastic deposits: notes on comparisons between fluvial and turbiditic systems. In: A. Taira and F. Masuda (eds.), Sedimentary Facies in the Active Plate Margin. Terra Scientific Publ. Comp., Tokyo, pp. 3-15.

Miall, A.D., 1996. The Geology of Fluvial Deposits. Springer Berlin, 582 pp.

Morton, A.C., 1985. Heavy minerals in provenance studies. In: G.G. Zuffa (ed.), Provenance of Arenites. D. Reidel Publication Comp., pp. 249-277.

Morton, A.C., 1991. Geochemical studies of detrital heavy minerals and their application to provenance research. In: A.C. Morton, S.P. Todd and P.D.W. Haughton (eds.), Developments in Sedimentary Provenance Studies. Geological Society, London, Special Publications, 57, pp. 31-45.

Morton, A.C. and Hallsworth, C., 1994. Identifying provenance-specific features of detrital heavy mineral assemblages in sandstones. Sedimentary Geology, 90, 241-256.

Morton, A.C. and Hallsworth, C.R., 1999. Processes controlling the composition of heavy mineral assemblages in sandstones. Sedimentary Geology, 124, 3-29.

Nehyba, S., Roetzel, R. and Maštera, L., 2012. Provenance analysis of the Permo-Carboniferous fluvial sandstones of the southern part of the Boskovice Basin and the Zöbing Area (Czech Republic, Austria): implications for paleogeographical reconstructions of the post-Variscan collapse basins. Geologica Carpathica, 63, 365-382. http://dx.doi.org/10.2478/v10096-012-0029-z

Nemec, W., 1988. The shape of the rose. Sedimentary Geology, 59, 149-152.

Nemec, W., 2005. Principles of lithostratigraphic logging and facies analyses. Institutt for geovitenskap, University of Bergen, 1-28.

Nemec, W., 2009. What is a hyperconcentrated flow? In: 27th IAS Meeting of Sedimentology, Alghero Italy, 20-24.09.2009, Abstract book. p. 267.

Nemec, W. and Muszyński, A., 1982. Volcaniclastic alluvial aprons in the Tertiary of Sofia district (Bulgaria). Rocznik Polskiego Towarzystwa Geologicznego (Journal of the Polish Geological Society), 52, 239-303.

Nemec, W. and Steel, R.J., 1984. Alluvial and Coastal conglomerates: Their significant features and some comments on gravelly mass-flow deposits. In: E.H. Kostner and R.J. Steel (eds.), Sedimentology of Gravels and Conglomerates. Canadian Society of Petroleum Geologists, Memoir 10, pp. 1-31.

Nesbitt, H.W. and Young, G.M., 1982. Early Proterozoic climates and plate motions inferred from major element chemistry of lutites. Nature, 299/21, 715-717.

Nichols, G.J. and Fisher, J.A., 2007. Processes, facies and architecture of fluvial distributary system deposits. Sedimentary Geology, 195, 75-90. http://dx.doi.org/10.1016/j.sedgeo.2006.07.004

Niedermayr, G., 1967. Die akzessorischen Gemengteile von Gföhler Gneis, Granitgneis und Granulit im niederösterreichischen Waldviertel. Annalen des Naturhistorischen Museums Wien, 70, 19-27.

Ohta, T., 2008. Measuring and adjusting the weathering and

hydraulic sorting effects for rigorous provenance analysis of sedimentary rocks: a case study from the Jurassic Ashikita Group, south-west Japan. Sedimentology, 55, 1687-1701. http://dx.doi.org/10.1111/j.1365-3091.2008.00963.x

Olsen, H., 1989. Sandstone-body structures and ephemeral stream processes in the Dinosaur Canyon Member, Moenave Formation (Lower Jurassic), Utah, U.S.A. Sedimentary Geology, 61, 207-221.

Partsch, P., 1843. Geognostische Karte des Beckens von Wien und der Gebirge, die dasselbe umgeben - oder - Erster Entwurf einer geognostischen Karte von Österreich unter der Enns mit Theilen von Steiermark, Ungern, Mähren, Böhmen und Österreich ob der Enns. K. K. Hof- u. Staats-Aerarial-Druckerei.

Partsch, P., 1844. Erläuternde Bemerkungen zur geognostischen Karte des Beckens von Wien und der Gebirge, die dasselbe umgeben. 24 pp.

Passchier, S., 2004. Variability in geochemical provenance and weathering history of Sirius group strata, Transantarctic Mountains: implications for Antarctic glacial history. Journal of Sedimentary Research, 74/5, 607-619. http://dx.doi.org/10.1306/022704740607

Passchier, S. and Whitehead, J.M., 2006. Anomalous geochemical provenance and weathering history of Plio-Pleistocene glaciomarine fjord strata, Bardin Bluffs Formation, East Antarctica. Sedimentology, 53, 929-942. http://dx.doi.org/10.1111/j.1365-3091.2006.00796.x

Pettijohn, F.J., Potter, P.E. and Siever, R., 1987. Sand and Sandstone. Springer, New York, 618 pp.

Pober, E. and Faupl, P., 1988. The chemistry of detrital chromian spinels and its implications for the geodynamic evolution of the Eastern Alps. Geologische Rundschau, 77/3, 641-670.

Poldervaart, A., 1950. Statistical studies of zircon as a criterion in granitization. Nature, 165, 574-575.

Pupin, J.P., 1980. Zircon and Granite Petrology. Contributions to Mineralogy and Petrology, 73, 207-220.

Pupin, J.P., 1985. Magmatic zoning of hercynian granitoids in France based on zircon typology. Schweizerische Mineralogische und Petrographische Mitteilungen, 65, 29-56.

Ramos, A. and Sopeña, A., 1983. Gravel bars in low sinuosity streams (Permian and Triassic, central Spain). IAS Special Publication, 6, 301-312.

Reid, I. and Frostick, L.E., 1987. Towards a better understanding of bedload transport. In: F.G. Etheridge, R.M. Flores and M.D. Harvey (eds.), Recent Developments in Fluvial Sedimentology. Society of Economic Paleontologists and Mineralogists, Special Publications, 39, 13-20.

Ritter, J.B., Miller, J.R., Enzel, Y. and Wells, S.G., 1995. Reconciling the roles of tectonism and climate in Quaternary alluvial fan evolution. Geology, 23, 245-248.

Roscher, M. and Schneider, J.W., 2006. Permo-Carboniferous climate: Early Pennsylvanian to Late Permian climate development of central Europe in a regional and global context. In: S.G. Lucas, G. Cassinis and J.W. Schneider (eds.), Non-Marine Permian Biostratigraphy and Biochronology. Geological Society, London, Special Publications, 265, pp. 95-136.

Roser, B.P. and Korsch, R.J., 1986. Determination of tectonic setting of sandstone-mudstone suites using SiO_2 content and K_2O/Na_2O ratio. Journal of Geology, 94, 635-650.

Roser, B.P. and Korsch, R.J., 1988. Provenance signatures of sandstone–mudstone suites determined using discriminant function analysis of major-element data. Chemical Geology, 67, 119-139.

Schermann, O., 1971. Bericht über die Neukartierung des Perms bei Zöbing (Blätter 21 und 38). Verhandlungen der Geologischen Bundesanstalt, 1971/4, A67-A68.

Schindler, T. and Hampe, O., 1996. Eine erste Fischfauna (Chondrichthyes, Acanthodii, Osteichthyes) aus dem Permokarbon Niederösterreichs (Zöbing, NE Krems) mit paläoökologischen und biostratigraphischen Anmerkungen. Beiträge zur Paläontologie, 21, 93-103.

Schumm, S.A., 1977. The Fluvial System. Wiley, New York, 338 pp.

Sensarma, S., Rajamani, V. and Tripathi, J. K., 2008. Petrography and geochemical characteristics of the sediments of the small River Hemavati, Southern India: Implications for provenance and weathering processes. Sedimentary Geology, 205, 111-125. http://dx.doi.org/10.1016/j.sedgeo.2008. 02.001

Shuster, M.W. and Steidtmann, J.R., 1987. Fluvial-sandstone architecture and thrust-induced subsidence, northern Green River basin, Wyoming. In: F.G. Ethridge, R.M. Flores and M.D. Harvey (eds.), Recent developments in Fluvial Sedimentology. Society of Economic Paleontologists and Mineralogists, Special Publication, 39, pp. 279-285.

Smith, S.A., 1974. Sedimentation in a meandering gravel-bed river: the River Tywi, South Wales. Geological Journal, 24, 193-204.

Sneh, A., 1983. Desert stream sequences in the Sinai Peninsula. Journal of Sedimentary Petrology, 53, 1271-1279.

Sohn, Y.K., Rhee, C.W. and Kim, B.C., 1999. Debris flow and hyperconcentrated flood-flow deposits in an alluvial fan, northwestern part of the Cretaceous Yongdong Basin, central Korea. The Journal of Geology, 107, 111-132.

Stanistreet, I.G. and McCarthy, T.S., 1993. The Okavango fan and the classification of the subaerial fan systems. Sedimentary Geology, 85, 115-133.

Stesky, R. M., 1998. Spheristat 2 for Windows 3.1, Users Manual. Pangea Scientific, Ontario.

Stur, D., 1870. Beiträge zur Kenntniss der Dyas- und Steinkohlenformation im Banate. Jahrbuch der k.k. Geologischen Reichsanstalt, 20/2, 185-200.

Suess, F. E., 1912. Die moravischen Fenster und ihre Beziehung zum Grundgebirge des Hohen Gesenkes. Denkschrift der k. Akademie der Wissenschaften, mathematisch-naturwissenschaftliche Klasse, 88, 541-631.

Tenchov, Y.G., 1980. Die paläozoische Megaflora von Österreich. Eine Übersicht. Verhandlungen der Geologischen Bundesanstalt, 1980/2, 161-174.

Todd, S.P., 1989. Stream-driven, high-density gravelly traction carpets: possible deposits in the Traberg Conglomerate Formation, SW Ireland and some theoretical considerations of their origin. Sedimentology, 36, 513-530.

Triebold, S., Eynatten, H. von, Luvizotto, G.L. and Zack, T., 2007. Deducing source rock lithology from detrital rutile geochemistry: An example from the Erzgebirge, Germany. Chemical Geology, 244, 421-436. http://dx.doi.org/10.1016/j.chemgeo.2007.06.033

Tunbridge, I.P., 1981. Sandy high-energy flood sedimentation - some criteria for recognition, with an example from the Devonian of S.W. England. Sedimentary Geology, 28, 79-95.

Turcq, B., Albuquerque, A.L.S., Cordeiro, R.C., Sifeddine, A., Simoes Filho, F.F.L., Souza, A.G., Abrão, J.J., Oliveira, F.B.L., Silva, A.O. and Capitãneo, J., 2002. Accumulation of organic carbon in five Brazilian lakes during the Holocene. In: J.-J. Tiercelin (ed.), Lacustrine Depositional Systems. Sedimentary Geology, 148, pp. 319-342.

Vasicek, W., 1974. Bericht 1973 über Aufnahmen im Perm von Zöbing auf den Kartenblättern Horn (21) und Krems (38). Verhandlungen der Geologischen Bundesanstalt, 1974/4, A114-A115.

Vasicek, W., 1975. Blatt 21, Horn. Geologische Aufnahme (Paläozoikum). Verhandlungen der Geologischen Bundesanstalt, 1975/1, A25-A26.

Vasicek, W., 1977. Perm von Zöbing. Arbeitstagung der Geologischen Bundesanstalt 1977, Waldviertel, 15.-20.Mai 1977, 16-18, 69-72.

Vasicek, W., 1983. 280 Millionen Jahre alte Spuren der Steinkohlenwälder von Zöbing. Katalogreihe des Krahuletz-Museums, 4, 15-50.

Vasicek, W., 1991a. Das Jungpaläozoikum von Zöbing. In: R. Roetzel (ed.), Geologie am Ostrand der Böhmischen Masse in Niederösterreich. Schwerpunkt Blatt 21 Horn. Arbeitstagung der Geologischen Bundesanstalt, Eggenburg, 16.-20.9. 1991, pp. 98-101.

Vasicek, W., 1991b. Das Jungpaläozoikum von Zöbing. In: D. Nagel and G. Rabeder (eds.), Exkursionen im Jungpaläozoikum und Mesozoikum Österreichs. Exkursionsführer der Österreichischen Paläontologischen Gesellschaft, pp. 1-21.

Vasicek, W. and Steininger, F.F., 1996. Jungpaläozoikum von Zöbing. In: F.F. Steininger (ed.), Erdgeschichte des Waldviertels. Schriftenreihe des Waldviertler Heimatbundes, 38, pp. 62-72.

Viseras, C., Calvache, M., Soria, J.M. and Fernández, J., 2003. Differential features of alluvial fans controlled by tectonic or eustatic accommodation space. Examples from the Betic Cordillera, Spain. Geomorphology, 50, 181-202. http://dx.doi.org/10.1016/S0169-555X(02)00214-3

Vohryzka, K., 1958. Geologie und radiometrische Verhältnisse in den jungpaläozoischen Sedimenten von Zöbing, N.-Ö. Verhandlungen der Geologischen Bundesanstalt, 1958/2, 182-187.

Waldmann, L., 1922. Das Südende der Thayakuppel. Jahrbuch der Geologischen Bundesanstalt, 72/3-4, 183-204.

Walker, R.G. and James, N.P., 1992. Facies Models. Response to sea level changes. Geological Association of Canada, pp. 1-380, Toronto.

Weissmann, G.S., Hartley, A.J., Nichols, G.J., Scuderi, L.A., Olson, M., Buehler, H. and Banteah, R., 2010. Fluvial form in modern continental sedimentary basins: distributive fluvial systems. Geology, 38, 39-42. http://dx.doi.org/10.1130/G30242.1

Wells, N.A. and Dorr, J.A. Jr., 1987. Shifting of the Kosi River, northern India. Geology, 15, 204-207.

Winter, J., 1981. Exakte tephro-stratigraphische Korrelation mit morphologisch differenzierten Zironpopulationen (Grenzbereich Unter/Mitteldevon, Eifel-Ardennen). Neues Jahrbuch für Geologie und Paläontologie, Abhandlungen, 162/1, 97-136.

Young, G.M. and Nesbitt, H.W., 1998. Processes controlling the distribution of Ti and Al in weathering profiles, siliciclastic sediments and sedimentary rocks. Journal of Sedimentary Research, 68/3, 448-455.

Youngson, J.H., Craw, D., Landis, C.A. and Schmitt, K.R., 1998. Redefinition and interpretation of late Miocene-Pleistocene terrestrial stratigraphy, Central Otago. New Zealand. New Zealand Journal of Geology and Geophysics, 41, 51-68.

Zack, T., Eynatten, H. von and Kronz, A., 2004a. Rutile geochemistry and its potential use in quantitative provenance studies. Sedimentary Geology, 171, 37-58. http://dx.doi.org/10.1016/j.sedgeo.2004.05.009

Zack, T., Moraes, R. and Kronz, A., 2004b. Temperature dependence of Zr in rutile: empirical calibration of a rutile thermometer. Contributions to Mineralogy and Petrology, 148, 471-488.

Zimmerle, W., 1979. Accessory Zircon from Rhyolite, Yellowstone National Park (Wyoming, U.S.A.). Zeitschrift der deutschen Geologischen Gesellschaft, 130, 361-369.

Zimmermann, U. and Bahlburg, H., 2003. Provenance analysis and tectonic setting of the Ordovician clastic deposits in the southern Puna Basin, NW Argentina. Sedimentology, 50, 1079-1104. http://dx.doi.org/ 10.1046/j.1365-3091.2003.00595.x

Zimmermann, U. and Spalletti, L.A., 2009. Provenance of the Lower Paleozoic Balcarce Formation (Tandilia System, Buenos Aires Province, Argentina): Implications for paleogeographic reconstructions of SW Gondwana. Sedimentary Geology, 219, 7-23. http://dx.doi.org/10.1016/j.sedgeo.2009.02.002

Zuffa, G.G., 1980. Hybrid Arenites: Their Composition and Classification. Journal of Sedimentary Petrology, 50/1, 21-29.

Zuffa, G.G., 1985. Optical analyse of arenites: influence of methodology on compositional results. In: G.G. Zuffa (ed.), Provenance of arenites. D. Reidel Publishing Company, pp. 165-189.

Received: 13 April 2015
Accepted: 10 august 2015

Slavomír NEHYBA[1)*)] & Reinhard ROETZEL[2)]

[1)] Institute of Geological Sciences, Faculty of Science, Masaryk University, Kotlářská 2, CZ- 611 37 Brno, Czech Republic;

[2)] Geological Survey, Neulinggasse 38, A-1030 Wien, Austria;

[*)] Corresponding author, slavek@sci.muni.cz